2016

Developments in and prospects for photocathodic and tandem dye-sensitized solar cells

Andrew Nattestad
University of Wollongong, anattest@uow.edu.au

Ishanie Perera
Monash University

Leone Spiccia
Monash University, leone.spiccia@sci.monash.edu.au

Publication Details

Nattestad, A., Perera, I. & Spiccia, L. (2016). Developments in and prospects for photocathodic and tandem dye-sensitized solar cells. Journal of Photochemistry and Photobiology C: Photochemical Reviews, 28 44-71.

Developments in and prospects for photocathodic and tandem dye-sensitized solar cells

Abstract
Third generation photovoltaics are based on the concept of providing high conversion efficiencies with low device production costs. As such, second generation concepts, such as Dye-sensitized Solar Cells (DSCs), serve as a good starting point for the development of these new devices. Tandem DSC devices are one example of such a concept, and can be constructed using two photoactive electrodes (one photoanode and one photocathode) inside the one cavity, increasing the theoretical efficiency limit by around 50% as compared to the conventional design. As there has been substantial effort devoted to the development of n-type DSCs, the focus of researchers investigating tandem DSCs has been to create high performance p-type systems, which operate by an analogous, but inverted, mechanism to n-type DSCs.

Disciplines
Engineering | Physical Sciences and Mathematics

Publication Details
Nattestad, A., Perera, I. & Spiccia, L. (2016). Developments in and prospects for photocathodic and tandem dye-sensitized solar cells. Journal of Photochemistry and Photobiology C: Photochemical Reviews, 28 44-71.

Developments in and Prospects for Photocathodic and Tandem Dye-sensitized Solar Cells

Andrew Nattestad
ARC Centre of Excellence for Electromaterials Science, Intelligent Polymer Research Institute, the University of Wollongong

Ishanie Perera
Department of Chemistry, Faculty of Science, University of Peradeniya, Peradeniya 20400, Sri Lanka.
and
School of Chemistry, Monash University, Clayton 3800, Australia

Leone Spiccia
School of Chemistry, Monash University, Clayton 3800, Australia

ABSTRACT

Third generation photovoltaics are based on the concept of providing high conversion efficiencies with low device production costs. As such, second generation concepts, such as Dye-sensitized Solar Cells (DSCs), serve as a good starting point for the development of these new devices. Tandem DSC devices are one example of such a concept, and can be constructed using two photoactive electrodes (one photoanode and one photocathode) inside the one cavity, increasing the theoretical efficiency limit by around 50% as compared to the conventional design. As there has been substantial effort devoted to the development of n-type DSCs, the focus of researchers investigating tandem DSCs has been to create high performance p-type systems, which operate by an analogous, but inverted, mechanism to n-type DSCs.

In order to realize high efficiency pDSCs a number of strategies have been pursued. Much of this has looked to optimizing individual components, such as the development of novel dyes with tailored absorption and electronic properties, the synthesis of new semiconductors and the incorporation of different redox mediators. Additionally, tandem devices require one to analyse the whole device, particularly to manage light harvesting across the two electrodes, which are intrinsically connected in series. Although this is a challenging task, it does open opportunities for more radical device redesigns.

GLOSSARY

APCE / IQE	Absorbed Photon to Charge Carrier Efficiency / Internal Quantum Efficiency
CB	Conduction Band
CE	Counter Electrode
E_G	Band gap
FF	Fill factor
HOMO	Highest Occupied Molecular Orbital
IPCE / EQE	Incident Photon to Charge Carrier Efficiency / External Quantum Efficiency
J_{SC}	Short Circuit Current Density
LUMO	Lowest Unoccupied Molecular Orbital
nDSC	Photoanodic Dye-sensitized Solar Cell
OPV	Organic photovoltaic
PCE	Photovoltaic Conversion Efficiency
pDSC	Photocathodic Dye-sensitized Solar Cell
PEC	Photoelectochemical Cell
pnDSC	Tandem Dye-sensitized Solar Cell (containing photoanode and photocathode)
pQDSC	Photocathodic Quantum Dot-sensitised Solar Cell
PV	Photovoltaic
$_qE_f$	Quasi Fermi energy / Quasi Fermi level
SOMO	Singularly Occupied Molecular Orbital
SQ	Shockley-Queisser (particularly with reference to predicted efficiency limits of single junction PV device)
VB	Valence Band
V_{OC}	Open Circuit Voltage
ΔG	Driving force
ΔG_{inj}	Driving force for charge injection
ΔG_{reg}	Driving force for dye regeneration

1. ORIGINS AND OPERATION OF PHOTOCATHODIC DYE-SENSITIZED SOLAR CELLS

1.1. OVERVIEW

The demand for low cost clean energy necessitates continued research and development into technologies capable of producing such forms of electricity. To date, Dye-sensitized Solar Cells (DSCs) have been able to attain solar-to-electric conversion efficiencies of over 14% [1]. This is still significantly lower than pn-junction silicon devices or methylammonium lead halide based devices, which have gained popularity recently [2]. DSCs do, however, offer the prospect of being cheap and scalable in production, including amenability to roll-to-roll processing, without the toxicity associated with some competing technologies (such as those that use Cd, Pb based materials). DSCs are also highly customisable, with molecular light harvesters which can be tuned to absorb different wavelengths; redox mediators and semiconductors that can control device voltages. The authors of this review, and anybody who has worked in this area, of course note that the reality of device development is not so trivial and the interactions between these components should not be underestimated.

This range of controllable parameters makes DSCs ideal candidates for "third generation" photovoltaic (PV) concepts. This third generation has been defined by Martin Green [3] as devices which can surpass the Shockley-Queisser limit [4] (a concept addressed below) and do so at a low cost. This category of device is described in opposition to (i) the first generation of pn-junction silicon and (ii) the second generation of, primarily thin film, low cost but low efficiency devices including a range of chalcogenide based materials, amorphous silicon, organic photovoltaics and, of course, dye-sensitized solar cells (DSCs).

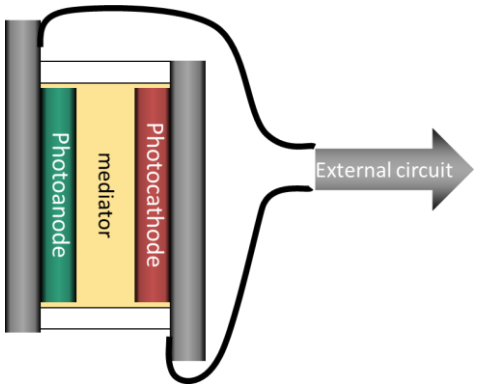

Figure 1 – A simplified schematic of a tandem pnDSC, comprised of a photoanode and photocathode, connected internally through a redox mediator as well as via an external circuit.

Here we discuss one implementation of a third generation concept, a tandem DSC (pnDSC) which incorporates a photocathode and a photoanode (shown schematically in Figure 1). Due to the configuration of such a device the attainable voltages (open circuit, V_{OC}) in the tandem device are nominally the sum of those in analogous photoanodic and photocathodic devices (nDSC and pDSC respectively), while current densities (J_{SC}) will be limited by the weaker of the electrodes, in accordance with Kirchoff's circuit laws. While efficiencies in excess of 8% are routinely reported for nDSC, to date the efficiencies of pDSCs are still much lower. Given the aforementioned circuit requirements, we will focus largely on the development of the pDSCs as this appears to be the biggest obstacle in the path of realising high efficiency pnDSCs (although, as we discuss later, there is a growing argument to look at redesigning the photoanode). Thus, interest in pDSC research is almost exclusively

with an aim towards incorporation in pnDSC. one major exception to this is, of course, the use of dye-sensitised photocathodes in water splitting applications, which is visited in more detail in Section 2.5.2.

A brief historical perspective on events leading up to the first pDSC report is provided, as well as an overview of their development since this time. Following on from this, the prospects for this technology are analyzed and possible avenues for continued improvement proposed.

1.2. A BRIEF HISTORY OF EVENTS LEADINGUP TO THE pDSC

This section highlights some of the most important developments in history of photovoltaic research with reference to the landmark development of the pDSC and pnDSC in 1999 and 2000, respectively [5, 6]. The story of human understanding of photovoltaics (PV) commences with the work of Edmond Bequerel [7], more than 175 years ago, when he observed a voltage arising from the exposure of silver halide electrodes to light, *i.e.,* a photoelectrochemical cell (PEC). It was the better part of a century until Einstein was able to formally explain the nature of this effect, in work that would lead to him being awarded the Nobel prize for physics 1921 [8]. In this intervening years researchers made further observations, including (of particular interest here) James Moser, [9] who reported the increased sensitivity of an electrode when Erythrosin was introduced. As such, this can be considered the first sensitized PEC.

Throughout the early to mid-20^{th} century there was comparatively little research into PEC systems, while pn junction photovoltaics became more established with Bell labs reporting 6% photovoltaic conversion efficiency (PCE) in 1954; a massive jump from the 0.5% of commercial photocells at the time [10]. On the other hand, interest in PEC research grew substantially during the late 1950's and 1960's, with fundamental principles of operation investigated by researchers, such as Nelson, Tributsch and Gerisher. [11, 12]. The field received a further boost in attention following the report by Honda and Fujishima [13] of photodriven water splitting using rutile titanium(IV) dioxide (TiO_2). As Nozik later commented, Honda and Fujishimas were "the first to point out the potential application of photoelectrochemical systems for solar energy conversion and storage" [14], representing a departure from purely fundamental studies into physical processes, towards application based PEC. Interestingly, as Honda and Fujishima observed oxygen evolution at the TiO_2 surface they actually mentioned the need for a p-type semiconductor to create a tandem device in order to realize the capabilities of such devices.

Five years later, Jeffrey Bolts and co-workers [15] were the first to realize a tandem regenerative PEC system, using n-CdSe and p-CdTe electrodes. In this case a polysulfide redox electrolyte was employed to provide a photovoltaic system rather than the provision of chemical energy storage (as in the conversion of water into molecular hydrogen and oxygen).

The concept of p-type sensitisation was highlighted by Memming 1972, using various dyes on both n- and p- doped GaP [16]. At this point there was still a significant debate between researchers as to the mechanism of photocathodic sensitisation, with models for either charge transfer or energy transfer presented - as reproduced below in Figure 2. In Memming's work charge transfer was shown to be at least the dominant (if not exclusive) mechanism.

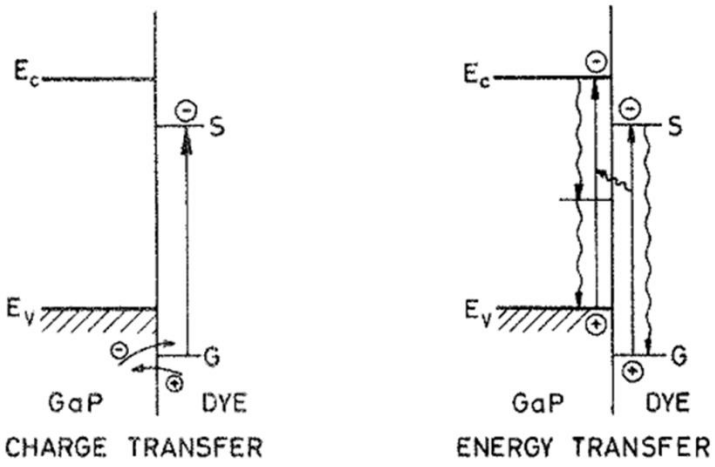

Figure 2 – Charge and energy transfer models, the two mechanisms initially proposed for photocathodic sensitisation – Reprinted with permission, from Memming - Photochemistry and Photobiology 16(4). Copyright 1972 American Chemical Society [16].

Nozik's 1978 review of the field, from which the above quote was taken, provides an excellent overview of the state-of-play in PEC research at the time, analysing the early fundamental studies, while setting up for the following decade of again increased interest in the concept of PEC and specifically sensitized PEC. In 1980 Matsumura *et al.* [17] provided a benchmark of 2.5% conversion efficiency under monochromated light (22% Incident Photon to Charge carrier Efficiency - IPCE) using an aqueous (iodine) electrolyte and sintered Al doped ZnO disk comprised of microparticles, stained with Rose Bengal. During the same period, Tennakone *et al.* [18-20] reported the p-type material CuSCN, sensitized by a variety of organic dyes.

The 1991 Nature paper of O'Regan and Gratzel was, of course, one of the most important developments in this field [21]. This was the first sensitized PEC to give a substantial device efficiency under broadband illumination (~7% PCE), and demonstrated that the nanoparticles could increase the effective surface area without leading to catastrophic recombination. This article has now been cited more than 15,000 times (Reuters Web of Science).

In 1995, O'Regan [22] also used the CuSCN, this time in a DSC, to transport holes away from oxidised dye molecules (after it having injected an electron into an n-type semiconductor such as TiO_2). Importantly, it was seen that this process could be very efficient (quantum efficiency ≤ 88%), however, it was only viewed as a way to replace the liquid electrolyte in a conventional DSC design, with O'Regan describing this device as a Dye-sensitized Heterojunction (DSH), meaning that it is not capable, even with ideal materials, to surpass the Shockley-Queisser (SQ) limit. Since this time, a range of p-type semiconductors have found use as hole transport materials in DSCs including CuO [23], CuSCN [22], $4CuBr{\cdot}3S(C_4H_9)_2$ [24], CuI [25], $CuAlO_2$ [26] and NiO [27].

In 1999 He *et al.* reported the first pDSC [5], followed by the incorporation of this photocathode a pnDSC the year after [6]. Here they employed either Erythrosin B or a free-base porphyrin as a sensitizer on a porous scaffold of Nickel(II) Oxide (NiO) nanoparticles, with an iodide/tri-iodide redox mediator. Upon illumination (68% sun) they observed pDSC device efficiencies of 0.0076% and 0.0033% respectively. The pnDSC device reported by He *et al.* [6] had a PCE of 0.39% and served as an important proof-of-principle, providing nearly additive V_{OC} as one might expect ($nV_{OC} + pV_{OC} \sim pnV_{OC}$). In this initial report the photoanode and photocathode were not optimised to produce matching current densities, which is to say the nDSC alone provided a J_{SC} of ~7 mA/cm^2, while the pDSC was only capable of producing J_{SC} ~0.27 mA/cm^2. In principle it can be expected that the *de facto* series connection of the electrode should limit the J_{SC} of a pnDSC to the lower of what the two

electrodes can generate. In actual fact the J_{SC} is higher but the current-voltage (J-V) curve displays an inflection (similar to the schematic in Figure 3 below). This suggests that at small applied biases (close to J_{SC}) the overpotential for electrolyte reduction at the cathode is sufficiently large that the system is driven by the photoanode. This phenomenon has also been observed by other authors when the photoelectrodes are not current matched [28, 29], but the maximum power point seems to inevitably reside in a voltage range where both photoelectrodes are the primary elements driving current flow (rather than dark processes).

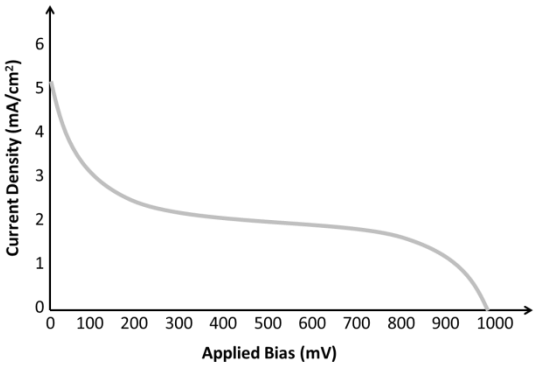

Figure 3 – Schematic of current-voltage response of pnDSC with poor current matching.

Developments in pDSC device efficiency are addressed below in Section 2.1 and show a rapid and dramatic increase since this first report. pDSCs have also been the subject of a number of review articles, including specialised topics such as ternary copper oxide materials [30-36].

1.3. DEVICE OPERATION

The photocathode (shown schematically in Figure 4a) consists of a p-type semiconductor to which with a dye is affixed. Upon photoexcitation this dye molecule is able to 'inject a hole' into the conduction band (CB) of the semiconductor. This hole (h^+) injection can also be viewed as an electron (e^-) being injected from the semiconductor to the dye, made possible by the dual Singularly Occupied Molecular Orbitals (SOMO) of the excited dye. After this charge transfer process, the resulting anionic dye is oxidised back to its neutral state by a redox active electrolyte. In a way somewhat similar to the debate about photocathodic sensitisation mechanisms during the 1960's and 1970's (see Figure 2), initially there was uncertainty about which process (h^+ injection to semiconductor or e^- to the mediator) occurred first. This was addressed by Borgström *et al.* [37] who were able to verify this ordering of these events in 2005, with the observation of dye anion spectral features following photoexcitation. The extracted hole travels through the mesoporous network of the p-type semiconductor to an external circuit and then the counter electrode, where it serves to oxidize the reduced species in the electrolyte, thereby maintaining charge balance. Typically, a catalytic material, such as platinum, is introduced on the counter electrode to minimize the required over-potential for regeneration in single photoelectrode devices. The attainable voltage (open circuit voltage, V_{OC}) of this pDSC is defined by the difference in energy of the redox mediator and the quasi Fermi energy ($_qE_F$) of holes in the p-type material (typically approximated to the VB edge). Although it is possible that $_qE_F$ can be depressed into the VB of a p-type semiconductor (or raised into the CB of a n-type material), very slow charge transport, in concert with very limited recombination, would be required to build up charge densities large enough to have a significant impact on V_{OC}. The maximum current density (short circuit

current density, J_{SC}) will depend upon light harvesting efficiency (LHE), charge injection and charge collection efficiencies (Φ_{inj} and Φ_{CC} respectively).

In comparison, for the nDSC case (Figure 4b), the photoexcitated dye injects an electron into the CB of an n-type semiconductor, which then diffuses through the mesoporous scaffold to the external circuit. The resultant dye cation can be reduced by the electrolyte, which is itself reduced at the counter electrode, by charges extracted at the working electrode. Once again catalytic materials, such as platinum, are used to expedite this process. Here, the V_{OC} is limited by ${}_qE_F$ of electrons in the n-type material and the redox potential of the electrolyte. The upper limit of J_{SC} is defined in the same way as above.

When both of the aforementioned systems are brought together their inverted mechanisms of operation serve as a compliment (Figure 4c). If charge generation is kept in balance (for the moment recombination processes are set aside from our considerations), the two systems will create a higher V_{OC} as they are, *de facto*, series connected, *i.e.* limited by ${}_qE_F$ of holes in the p-type and electrons in the n-type semiconductor. J_{SC} is nominally limited to the lower of the two photoelectrodes, however, as was highlighted above (Figure 3), this is not strictly true.

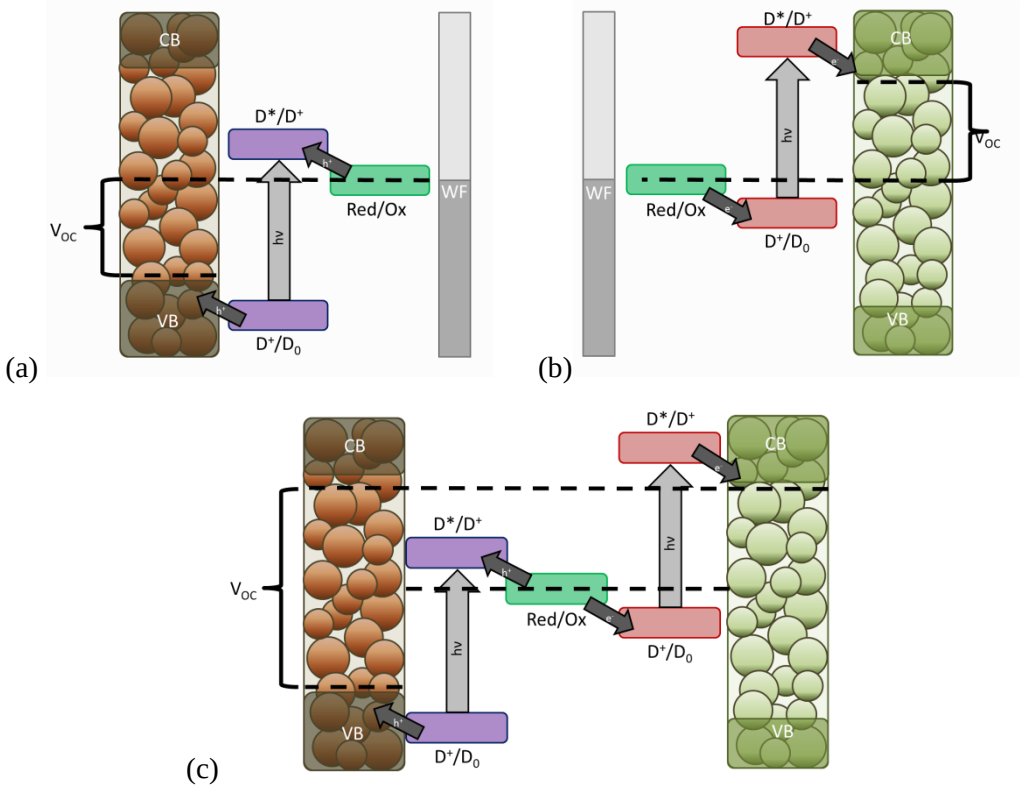

Figure 4 – Schematic operation of (a) photocathodic pDSC, (b) photoanodic nDSC and (c) tandem pnDSC.

The above description of device operation focussed solely on the pathways which lead to measurable electrical output (*i.e.* the ideal pathway). It is important to realize that in real devices recombination reactions compete with the forward processes (shown schematically in Figure 5). The primary recombination mechanisms in pDSCs are back transfer of injected holes from the valence band (VB) of the semiconductor to either the anionic dye or to the oxidised species in the electrolyte.

Early studies saw the former of these mechanisms to be a major limitation with a substantial portion of the injected charges being rapidly lost in recombination reactions [37, 38]. Fortunately, it has been possible to create systems where these recombination reactions are sufficiently retarded that high quantum efficiencies have

been realized [28, 39]. The most effective method for achieving this has been the tailoring of sensitizers, although the use of core-shell structured working electrodes has also been shown to be moderately effective [40, 41]. Both of these approaches are discussed in greater detail below, in Sections 2.2 and 2.4.3 respectively.

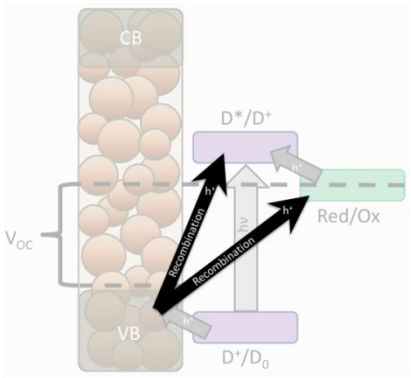

Figure 5 – Schematic representation of major recombination pathways in pDSCs.

1.4. THIRD GENERATION PHOTOVOLTAICS

As mentioned in Section 1.1, pnDSCs can be considered an example of a third generation photovoltaic concept. The definition provided by Martin Green [3] suggests three labels for photovoltaics. The first generation includes the first commercialised technology, pn-junction silicon. From the Bell labs 1954 report of 6% conversion efficiency, confirmed values have now exceeded 25% [2] even under non-concentrated sunlight conditions. Given that these are single junction devices with a band gap of ~1.1 eV, these efficiencies are close to their theoretical upper limit.

The second generation is defined as being a low cost alternative to the above. It was initially envisaged that thin film technologies would replace crystalline silicon solar cells in many applications due to reduced manufacturing costs. To date the only non-silicon based system to see significant commercial adoption is cadmium telluride (CdTe). Reasons for this include the continued decrease in cost of crystalline silicon PV and the proportion of a systems total price which is accounted for by 'balance-of-plant' costs. Meanwhile, some other second generation technologies have found niche markets, such as amorphous silicon panels on calculators and DSCs integrated into backpacks where they can be used to charge portable electronic devices [42].

Technologies which offer the prospect to surpass the efficiency limits set by a single junction have been termed the third generation. Ideally, this improved performance should also be achieved without significant increase to the cost, although the above example of pn-junction silicon reminds us the role of continued development, improved production processes and economies of scale play in achieving this. Before looking at examples of these third generation devices, it is important to understand where the limiting efficiencies for single junction devices come from.

1.4.1 EFFICIENCY LIMITATIONS IN SINGLE JUNCTION PV

Photons emitted from the sun, reaching the surface of the earth, cover the range of ~280-4000 nm, (4.4 eV < hν < 0.31 eV), with their distribution reported under different conditions, such as air mass 1 (AM1) corresponding to the sun being directly overhead. In order to better approximate typical illumination conditions,

AM1.5 is more commonly used as a standard, *i.e.* the distribution of photons in sunlight under 1.5 air masses, equivalent to irradiation from the sun while it is angled at of 37°, at 41.81° from the zenith [43].

If photons are more energetic than the bandgap (E_G) of a semiconductor they can be absorbed, with their energy used to excite an electron from the VB to the CB, thus providing an electron-hole pair (exciton). In most cases any excess energy ($h\nu > E_G$) is simply lost as heat. Photons of lower energy than E_G are simply transmitted and their energy lost to the PV device. This highlights the trade-off of absorbed photons (which controls current) and exciton energy (voltage), in a simple and generalised sense. It also demonstrates the role E_G plays in determining the attainable efficiency for a particular material. In 1963, Shockely and Queisser published a detailed balance account of this [4], also accounting for radiative recombination. In their analysis, the sun was assumed to be a perfect 6000 K black body irradiation source (as opposed to a measured solar spectrum) while the device is held at 300 K. From this they estimated a single junction efficiency limit of ~30 % for a 1.1 eV E_G for non-concentrated sunlight. As a result, the limiting efficiency of a device based on its E_G is referred to as its Shockley-Queisser (SQ) limit.

Henry [44] revisited this topic, using both a measured solar spectrum and also looking at the possibility of using multiple junctions to better utilize the incident light. A generalised schematic of a tandem solar cell (as compared to the specific case of pnDSCs shown in Figure 4c) can be seen below in Figure 6 and demonstrates how two junctions can each harvest different wavelength ranges, resulting in less energy being lost to thermalization in each. These electrodes can be connected in series or parallel, with a series connection typically preferred on account of the difference in device voltage - one way around this is to have two of the second electrode (low V_{OC}) in series (side-by side) in series with the first (high V_{OC}). Ideally, a series connected device would produce similar currents from each electrode (taking into account light transmission through the first electrode).

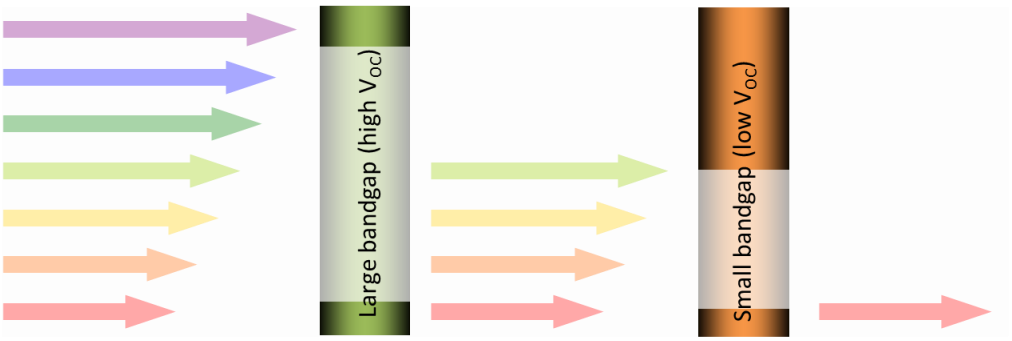

Figure 6 – Generalised schematic representation of a tandem solar cell, with each junction selectively harvesting one portion of the solar spectrum and converting it with high efficiency (comparatively small losses to thermalization).

As a result of this, two junction model (and the use of a more accurate solar spectrum) an efficiency limit of 41% for a tandem under 1 sun illumination (50% at 1000 suns) was calculated. For reference, Henry places the theoretical efficiency limit at 31% (37% for concentrated light) for a single junction, while a near infinite (36 electrode) configuration, under concentrated irradiation, provides a value of 72%.

The above models are based on pn-junction devices. While some authors have considered the cases of PEC [45] and others have specifically focussed on detailed balance accounts of organic sensitized systems, [46] the physical realities of DSCs leave a certain ambiguity as to the applicability of these models. Snaith [47] also presented an approach to determine the efficiency limits of DSCs, using a more empirical approach. Once charges

are injected into a wide bandgap material, the role of radiative recombination should become almost insignificant. However, the driving force required for this injection to occur efficiently and without substantial back-transfer is a loss in potential that must be minimised in order to realise high PCEs. In Section 3.2, we attempt to address the theoretical limits for pnDSC.

While multiple junction devices (particularly tandems) are the best developed and understood of the technologies capable of surpassing the above SQ limit, there are a number of approaches that can also make more effective use of sunlight as compared to the aforementioned single junction devices. This includes spectral modification (up-conversion / down-conversion) and their non-radiative counterparts (intermediate band and multiple exciton generation respectively) as well as hot carrier solar cells. For reference each of these is described briefly below in Table 1:

Table 1 – General overview of third generation PV concepts, with particular reference to implementations in DSCs.

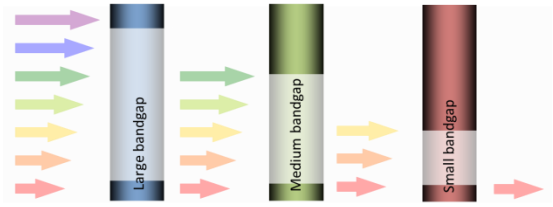

Multiple junction solar cell

Junctions arranged in decreasing order of E_G, resulting in small thermalization losses at each junction as the incident photons are only slightly more energetic than each E_G. A variant of this uses spectral splitting (*eg.* Dichroic mirrors, diffraction gratings or prisms) to irradiate side-by-side devices with wavelengths of light to which they are most suited.

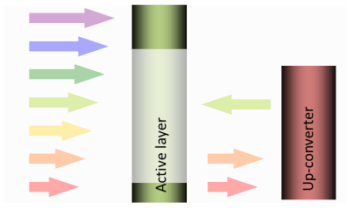

Photon up-conversion

The energies of two low energy photons, transmitted through the active layer, are combined and re-emitted back towards active layer. May be accomplished through sequential absorption, stimulated emission or triplet-triplet annihilation [48]. Allows for increased photocurrent generation without compromise V_{OC} [49, 50].

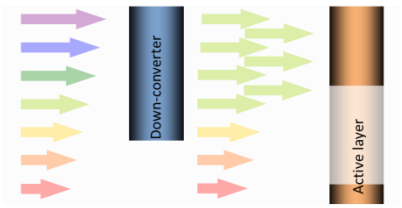

Photon down-conversion

High energy photons are able to excite a material which then emits multiple low energy photons. These can be absorbed by a low E_G material, resulting in higher J_{SC}. One example of this is singlet fission, the inverse of the triplet-triplet annihilation process.

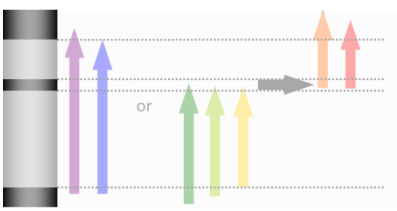

Intermediate band solar cell

Non-emissive analogue of an up-conversion system. Electrons can be either directly excited from the CB to VB by high energy photons or in a two stage process using an intermediate band (IB). (CB → VB or VB → IB and IB → CB). Recently the IB concept has been applied to DSCs [51, 52].

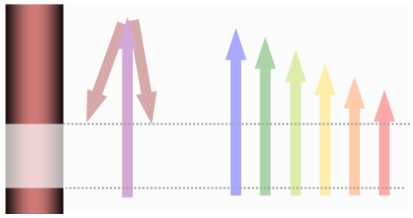

Multiple exciton generation

Non-radiative analogue of down-conversion. Certain materials, particularly quantum dots, can generate multiple excitons when excited by photon $h\nu > 2 \cdot E_G$ [53].

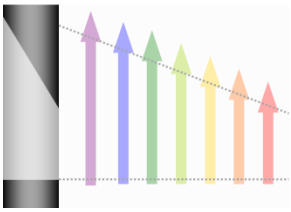

Hot carrier solar cell

Charges are extracted without being allowed to thermalize to the band edges. Allows for more energy to be extracted from high energy photons without transmissive losses of low energy ones, as a wide E_G material leads to.

As mentioned previously, the low projected cost, along with the design flexibility of DSCs, make them ideal candidates for use as the basis of third generation PV. To date there have been a number of examples of such, including up-conversion assisted, multi-exciton and recently an intermediate band dye-sensitized solar cell (see references in Table 1 above), as well as other variants of tandem (listed below in Table 2).

Table 2 – Various implementations of tandem DSC (aside from pnDSC)

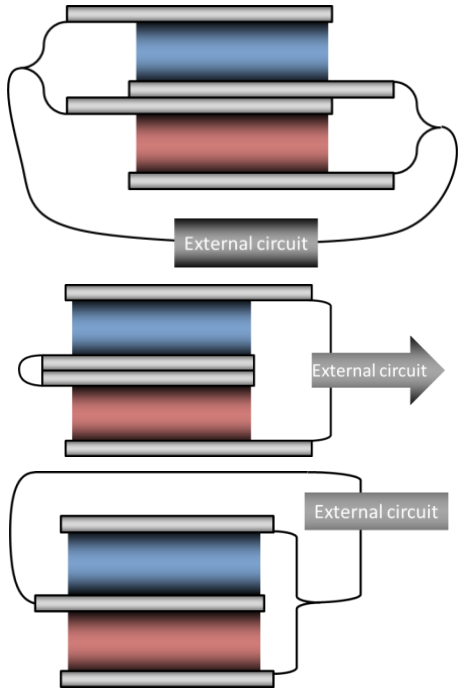

Stacked (nnDSC)

Two nDSCs stacked on top of one another, with the top being highly transmissive and the bottom employing a red-IR absorbing dye. The use of different redox mediators and/or semiconductors allows this device design, in principle, to surpass the single junction SQ limit.

First reported in 2004 [54, 55], this architecture has been employed to realize 11.5% conversion efficiency using spectrally complimentary organic dyes [56]. These can be configured either in series or in parallel.

Murayama and Mori introduced a similar concept incorporating a single mesh counter electrode into a DSC with two photoanodic working electrodes [57]. If different dye/semiconductor combinations are used on each of these electrodes, the system can, in principle, exceed the SQ limit.

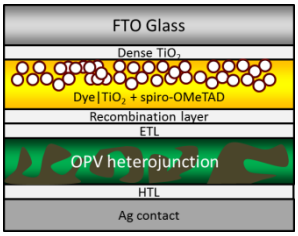

Hybrid (DSC + other)

Several attempts have been made to combing DSCs with other PV technologies better suited to the harvesting of infrared light. This has to date included CIGS [58] and organic systems [59].

2. pDSC LITERATURE SURVEY

It is arguable that development in that the field of nDSC has been hamstrung by the initial efficiencies reported by O'Regan and Grätzel in 1991 (and 10% published shortly after in 1993). Development of devices, such as DSCs, has often been characterised by researchers focussing on one component at a time, while rest of the device remained as per the state-of-the-art. It is questionable as to whether this is necessarily the best approach to device development. On one hand, the interaction between components in systems such as DSCs plays a significant role in determining their overall performance, while on the other, changing multiple parameters simultaneously increases the workload significantly. Systems including TiO_2, ruthenium sensitizers and iodide-triiodide redox mediators have been the standard for a long time, with departures from this formula (typically one component at a time) leading to lower overall PCE.

In 2006, a record PCE of 11.1% was set [60] and in 2010, 11.7% [61], with devices which again used a Ru complex sensitized, mesoporous TiO_2 and an I^-/I_3^- based electrolyte. Although issues with each component had been identified (Ru dyes are expensive and laborious to purify, iodine is corrosive and provides parasitic absorption) it was not until recently that this 'stalemate' was broken, notably with the work of Yella *et al.* [62], where the combination of a (Co(II)/(III)) redox mediator and Zn-porphyrin dye led to the realisation of 12.3% PCE. Further modification of the dye structure lead to 13% conversion efficiencies [63], while more recently 14.3% PCE has been realised using two organic dyes and a (Co(II)/(III)) mediator [1]. In a further departure from the conventional design, one of the two sensitizers used here was bound to the TiO_2 by a silyl anchoring group.

The impressive initial reported PCEs of nDSC were not mirrored in pDSCs. Their modest starting point (< 0.01%) may in some ways be seen as a benefit, pushing researchers to investigate all aspects of the device, and not necessarily in isolation [64-66]. It is obvious that more 'tweaking' the system will not achieve the target performance. Furthermore, general understanding of the science, garnered from work on nDSC has been able to feed into pDSC development.

When considering the design of a tandem, pnDSC, structure there needs to be even further emphasis placed on understanding of the interplay of components. This includes the need for an appropriate choice of redox mediator (with an understanding of dye-mediator interactions on both sides of the cell) and considerations of spectral matching. Furthermore, spectral matching for an optimised device needs to accommodate any parasitic absorptions which may occur due to the electrolyte or semiconductors. This is exemplified by the dramatically different performances of tandem devices under illumination from either the photoanode or photocathode side [28]. In addition to these special considerations, 'normal' DSC concerns still apply, such as volatility of electrolytes and sealing, corrosive mediators and the photodegradation of organic materials [67].

2.1. OVERVIEW OF pDSC DEVELOPMENT

In order to understand where the field of pDSC research sits at this point in time, three publication metrics (based on Reuters Web of Science searches) were examined here (Figure 7); specifically the distribution of these over the last 16 years. Firstly, citations of the 1999 paper from He *et al.* [5] were examined, as it is assumed that the field is small enough that the majority of relevant articles will still reference this work. This metric also includes a number of tangentially related articles, such as those using NiO for other purposes, where there is passing mention of its applicability in pDSCs. The second search looked at the number of articles which match the search term "photocathod*" and "dye sensiti* solar cell", with wildcards used to ensure variations are included. This search captures a more specific subset of papers, including review articles, but many of them may only include a small section on pDSC research. The third category was generated by us, based on papers we could find reporting original pDSC device data. Each of these categories shows the interest in this field in slightly different ways and of course all are important. It is noteworthy that there was a substantial lag from the first report (1999) and substantial interest from other researchers. This may have been due to a pessimistic outlook of the technology, given the low device conversion efficiencies.

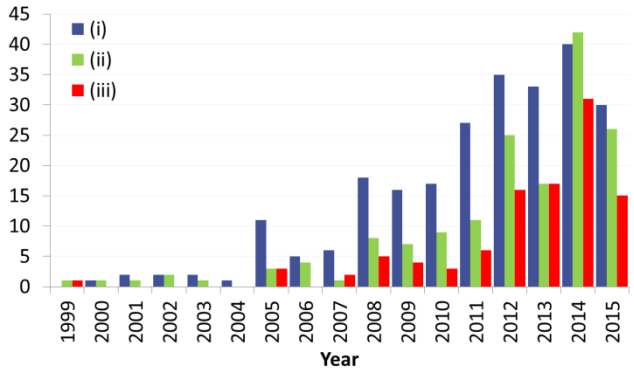

Figure 7 – Metrics for ISI indexed publications which (i) cite (He, et al 1999), (ii) contain the key words "photocathod*" and "dye sensiti* solar cell" or (iii) report original research data for pDSC devices.

The first paper on pDSCs, as discussed above, reported only very low efficiencies [5]. The next report on pDSC did not appear for another 6 years, when Nakasa *et al.* applied Coumarin 343 (C343) as a sensitizer [29]. Once some improvements were realised there appears to have been a snowball effect, with higher efficiencies attracting more attention, leading to more research being conducted, and subsequently further increases in device performance. Interest in pDSC may also be partially due to the crowded nature of nDSC research and the desire of researchers to find niche areas of research in which they can potentially have a greater impact. Until recently, with the commercial availability of dyes specifically designed for pDSCs [68], C343 sensitized NiO remained the 'unofficial standard' for photocathodes, used as a control in a number of studies [69-79].

In 2008, Morandeira *et al.* produced the first push-pull dye specifically tailored for pDSC application. In spite of a high (~45%) Absorbed Photon to Charge carrier Efficiency (APCE), low light harvesting efficiency limited overall performance [80]. The same year, members of the same group reported the dye "P1", with 0.05% conversion efficiency [81]. With further device optimisation this was increased to a PCE of 0.15% [82]. The structures of these dyes, along with other notable examples can be found in Table 3.

In 2010, our group introduced another donor-acceptor type dye, with a variable length bridge of alkylated thiophenes [28]. This served to substantially retard recombination between injected holes in the NiO and the dye anion, as evidenced by the long lived dye anion (observed in transient absorption measurements) and an APCE of ~96%, when six thiophene units are included. This was used to produce devices with up to 0.41% conversion

efficiency. The following year the replacement of commercial NiO with high crystallinity, faceted particles, lead to an increased V_{OC} and hence another record efficiency [83]. In 2012, and again in 2014, the substitution of I^-/I_3^- redox couple for (Co(II)/(III)) and then Fe(II/III) complexes resulted in PCEs of 1.3% and 2.51% respectively [84, 85], with devices displaying V_{OC}s comparable to those of high performance nDSCs. The last four of these record pDSC PCEs have been obtained using PMI-6T-TPA (Table 3).

In the sections, below we summarize work undertaken in the development and optimisation of pDSCs. This has been broken down into sections focused on sensitizers, electrolytes and semiconductors, in the interests of simplicity and readability. Once again it should be iterated that in the development of these devices everything should be (and sometimes is) 'on the table'.

2.2. SENSITIZERS

One of the most widely investigated components of pDSC (and nDSC for that matter) is the sensitizer - by our count there have been > 90 different sensitizers reported to be used in pDSCs to date. Some of the requirements for photocathodic and photoanodic systems are the same, such as chemical robustness and having a high extinction coefficient. Obviously the oxidation and reduction potentials need to provide sufficient driving force for charge injection into the semi-conductor, while mitigating back transfer. The exact magnitude of this is a debated topic, and is further discussed below in Section 3.2 where we attempt to estimate upper limits on pnDSC efficiencies.

Much of the early work in this field utilised 'off-the-shelf' dyes, such as Erythrosin B and C343. Use of the latter to sensitize photoanodes provides IPCE > 80% [86], and also facilitated high IPCE (> 20%) in pDSC devices [75]. A major challenge in the early stages of pDSC development was to prove that high quantum efficiencies could be realised at all. Mori *et al.* compared a series of sensitizers for p-DSCs including a C343 and another coumarin sensitizer, NKX-2311, which has a red-shifted absorption spectrum compared to C343. In spite of this red-shift, the J_{SC} was found to be lower than that of the devices made with C343 [75]. Cyanine sensitizers, NK-2684, NK-3628, and NK-2612, were also used in this comparative study, which led higher J_{SC} values, largely due to the higher absorption coefficient of these sensitizers. Device performance was severely limited by the interfacial charge recombination reactions occurring between the reduced sensitizer and the injected holes.

Table 3 - Selected structures of dyes used in pDSCs

Dye	Significance
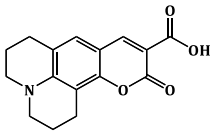 Coumarin 343 (C343)	One of the first dyes applied in pDSCs [29]. Commercially available and low cost. High IPCEs reported using this dye in both pDSC and nDSC devices.
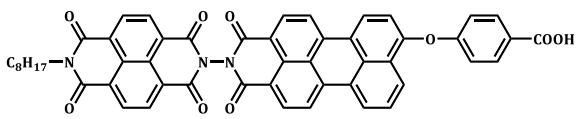 Peryleneimide–Napthalenediimide dyad (PI-NDI)	First donor-acceptor dye specifically designed for pDSC[80].

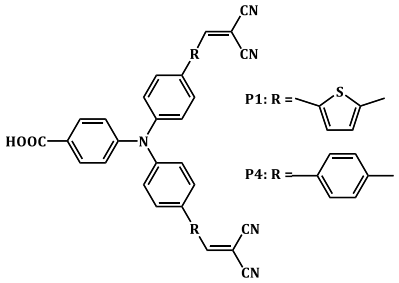

P1, P4

Breakthrough dyes, providing high APCE and IPCE [39, 81]. P1 is now commercially available [68].

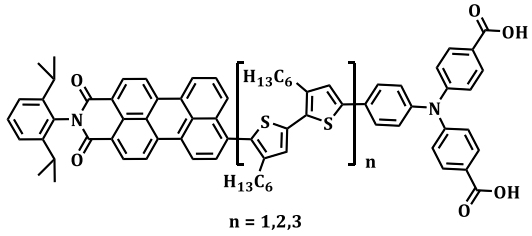

PMI-nT-TPA

Long lived charge separated state (TAS); high V_{OC} for I^-/I_3^- and NiO. Utilised in several successive champion pDSC devices [28, 83-85]. Synthesised by group of Peter Bäuerle.

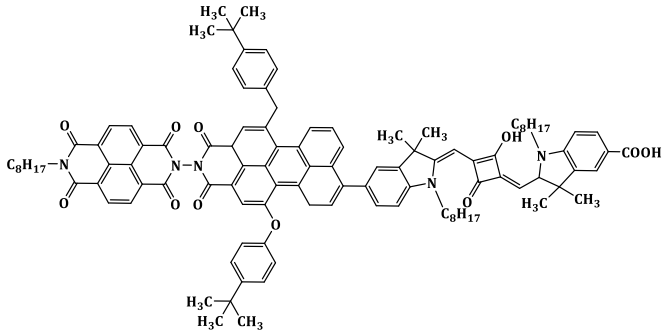

SQ-PMI-NDI

One of the most successful dyes to sensitize pDSC into the IR. A 25% IPCE was achieved at 620 nm [87].

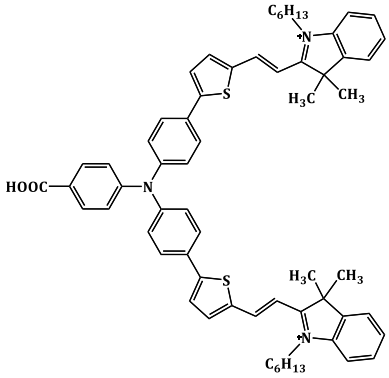

CAD3

Reported J_{SC} = 8.2 mA/cm^2. IR absorber; IPCE at 700 nm > 20% [88].

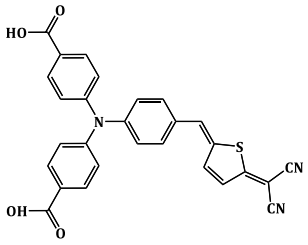

QT-1

Reported J_{SC} = 8.2 mA/cm^2 by Zhang *et al.* [89]. Structurally similar to the "O2" dye (*N.B.* Devices with O2 only obtained J_{SC} of 1.43 mA/cm^2 [90]).

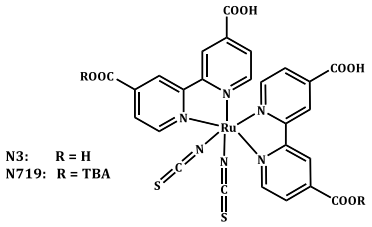

N3, N719

Staples of research for nDSC. Shown to have desensitizing effects when used in NiO pDSC [76]. Reported J_{SC} = 8.35 mA/cm^2 on $NiCo_2O_4$ [91].

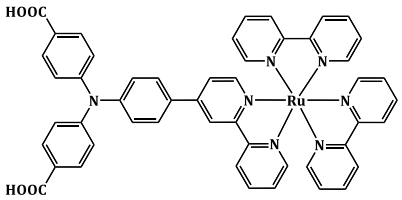

O3

Ru dye used to generate J_{SC} > 3 mA/cm^2 in pDSCs [92].

2.2.1 DONOR-ACCEPTOR TYPE DYES

At the most basic level, successful design of dyes for pDSC has involved the creation of donor-acceptor dyes, where two moieties are in electronic communication, but retain certain characteristics of their own. One of these moieties should be more electron withdrawing and the other electron accepting. In order to predict how such a molecule might perform when photoexcited, electron distribution in the highest occupied molecular orbital (HOMO) and lowest unoccupied molecular orbital (LUMO) are often calculated (HOMO-1 and LUMO+1 may also considered). The LUMO is considered as a good approximation of where the Single Occupied Molecular Orbital (SOMO) within which electron density generated following photoexcitation lies. such as is highlighted in the example in Figure 8. The LUMO should be characterized by low electron density in proximity to the surface, while the HOMO the opposite. This increases the probability of hole injection to the semiconductor, as well as promoting dye anion regeneration.

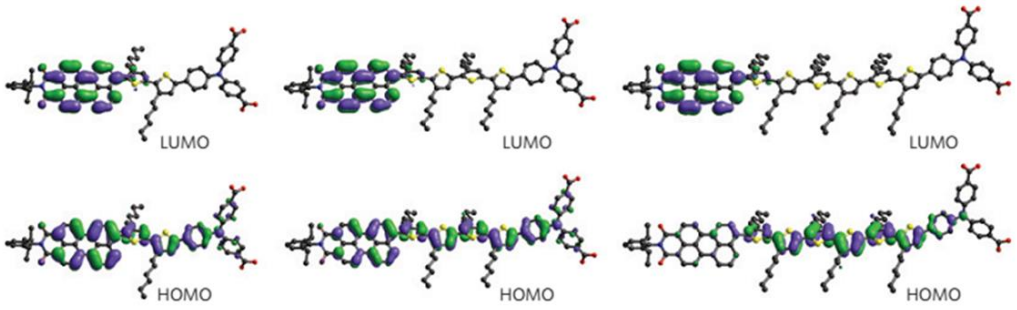

Figure 8 – Electron density in frontier orbitals of donor-acceptor dyes 'PMI-nT-TPA'. Originally published in Nature Materials [28], copyright Nature Publishing Group 2010.

The first dye explicitly designed (to our knowledge) for application in pDSCs, introduced by Morandeira *et al.* [80], was essentially a dyad containing perylene imide and naphthalene diimide moieties (PI-NDI). These researchers recognised that the rules for good dye design should be largely reversed compared to those for nDSC [93]. Although the concept of donor-acceptor dyes was initially borrowed from nDSC research, the necessity to

adopt these concepts in pDSC was much more pronounced, in part due to the effectiveness of dyes such as N719, which mitigated the necessity for such design in nDSCs for a long time. The more recent trend to move away from expensive and difficult to purify dyes in nDSC did however increased the demand for deeper understanding of these 'rules' for dye design.

As mentioned, one of the first dyes shown to provide reasonable J_{SC}s (at least within an order of magnitude of the record nDSC values) was "P1" (Table 3), which consists of a triphenylamine donor group and a dicyanovinylene acceptor group, connected via a thiophene ring [81]. Following device optimisation, a maximum IPCEs of 35% and then 63% were obtained by the same authors [39, 82]. A 44% IPCE was reported for a new dye, P4, alongside the value of 35% for P1. This new dye was produced by substitution of the two phenyl rings with thiophenes [39]. The PMI-nT-TPA series of dyes, first published in 2010, are composed of a perylenemonoimide group (PMI) acceptor, an oligothiophene spacer (nT, where n = 2, 4, 6) and are coupled to a triphenylamine group as the donor (TPA). These led to even higher efficiencies [28], with the systematic variation in the number of thiophene units resulted in the observed dye anion lifetimes in a redox free environment increasing by roughly an order of magnitude, as measured in transient absorption experiments. The variant with six thiophene units exhibited the longest-living charge-separated state and significantly enhanced device performance.

While the first donor-acceptor dyes were based on perylene imide and naphthelene diimide, the majority of reports since have incorporated either diphenylamine or triphenylamine as a donor moiety, most likely following reports of P1 and PMI-nT-TPA [28, 81]. Researchers have focused their attention towards testing a range of acceptors, various π-bridges as well as binding moieties. The creation of dye series with different acceptors has become a popular topic of study, with a number of groups [82, 94-96] exploring this aspect. Unfortunately, to date, none of these were able to provide improved performance over the aforementioned P1 and PMI-nT-TPA dyes, with the exception of P4 which provided slightly higher PCE than P1 in direct comparisons. Among the acceptors trialled were 9,10-dicyanoacenaphtho[1,2-b]quinoxaline (DCANQ), dicyanovinylene (DCV) [81, 90, 94-97], tricyanofurane [94] squarine [87, 94], bodipy [98] and 1,3-diethyl-2-thioxodihydropyrimidine-4,6-dione (DETB) [82, 96].

Some of the reasons put forward for the failure to further improve PCE were decreased driving forces for charge injection and/or dye regeneration (ΔG_{inj} and ΔG_{reg} respectively) depending on the moiety employed. Li *et al.* [99] recognised, the asymmetric rates of injection and regeneration suggest a smaller ΔG_{inj} should be required as compared to ΔG_{reg}. Furthermore, the nature of regeneration via a radical iodine intermediate ($I_3^- + e^- \rightarrow I_2^{\bullet-} + I^-$) means that the relevant value of ΔG_{reg} is actually ~ 325 meV smaller than the estimate often used (based on D^*/D^- and I^-/I_3^-) [82, 94, 100], and this needs to be accounted for. This translates to a substantial energy loss between that of the absorbed photon and what is outputted by the device. This issue is addressed again below in Sections 2.3.1 and 3.2.

To facilitate a long lived charge separated state, an extended π conjugated bridge is employed. In our 2010 study, we showed a sexthiophene bridge with near unity APCE [28]. In follow up studies, steric hindrance resulting from the location of the alkyl chain on the thiophene was shown to significantly affect the structure of the molecule and subsequently its electronic properties [101]. The twist between bridge and acceptor induced by the alkyl chain is seen to be important in promoting injection and/or preventing rapid recombination of the excited electron with holes in the semiconductor. Other groups have compared bridges comprised of thiophene [90, 96], carbazole [96], thiolated carbazole [96], pyridine [102] ethylenedioxythiophene (EDOT) [90], phenyl [90], fluorene [103], and combinations of the above [103].

In further studies by Le Pleux *et al.* [104], coupling of the PMI moiety to a naphthelenediimide (NDI) or a fullerene (C_{60}) as a secondary acceptor was found to increase the charge separated state lifetime by about five orders of magnitude compared to parent PMI sensitizer alone. Nevertheless, these modifications were not sufficient to surpass the performance achieved with the PMI-6T-TPA sensitizer.

2.2.2 DYE BINDING MECHANISM

As mentioned above, much of the development of dyes for pDSC looks at creating derivatives of either P1 or PMI-nT-TPA (or combining aspects of each) [105]. One of the major differences between these two benchmark dyes is the number of binding groups. On one hand, a single linker more readily facilitates inclusion of a second acceptor on TPA (either symmetric or asymmetric). This is particularly relevant for pDSC using NiO or other highly coloured semiconductors, as high LHE can be achieved with comparatively thin films, thereby limiting parasitic absorption. On the other hand, Chang *et al.*[106] found, from a direct comparison of mono- and di-carboxylated dyes with otherwise the same molecular structure, that the PCE of the device with the dicarboxylate linker was almost double that of the single. Similar redox potentials were observed but there was a major difference in dye loading. Therefore, they concluded that the inclusion of two binding groups forces the dyes into an upright configuration so that they are more densely packed and maintain photoexcited electrons further from the semiconductor.

Most dyes contain carboxylic acid linkers (or close relatives of), almost by default, as they have been widely used in nDSC, providing good chemical stability, reasonable injection and (typically) low back electron transfer rates. Interestingly, the recent record efficiency for nDSC was set using a cocktail system where one of the dyes employs a silyl anchor. Yann Pellegrin *et al.*[107] synthesized a ruthenium(II) tris(bipyridine) derivative with various linker groups, finding similar performances for carboxylate and catechol linkers, a slight improvement with methyl phosphinic acid and a substantially worse performance with biscarbodithioic acid. Notably, they also observed that the binding of carboxylic acid to NiO is ~18 times stronger than on TiO_2. A 2012 computational study of these dyes by Anne *et al.* [108], concluded these results were likely due to the dye redox potentials, which were dependent on the binding group. A similar study by Munoz-Garcia in 2015[109], using C343 as a model, saw similar shifts in calculated oxidation potentials when a carboxylic acid compared to a phosphonic acid. Although not advantageous here, this may be a method to stabilize dye frontier orbital energies, which will become necessary as NiO is replaced with other p-type semiconductors possessing more low lying VB edge potentials (vacuum scale). Furthermore, acetylacetone [87] and pyridine [102] have each been used to bind dyes to NiO. In early work on sensitized p-type materials, Tennakone used ionic binding to adhere dyes to CuSCN [19].

2.2.3 RUTHENIUM BASED SENSITISERS

While Ru dyes have been the dominant choice for sensitisation in photoanodes since the 1991 Nature article [21], their use in pDSCs has been limited. Several groups have reported the performances of pDSC devices using either N3 or N719, with mixed results. He *et al.* [71] observed a J_{SC} of 0.35 mA/cm^2, which is modest, compared to the 1 mA/cm^2 they measured from a C343 sensitized analogue and similar to what is observed by Sheehan *et al.* [110]. Here they also observed similar J_{SC} for their unsensitized device, suggesting that either electrolyte sensitization or measurement artefacts are the most likely cause of such current densities. Ursu *et al.* [111] applied N719 to $CuGaO_2$ and Fe-doped $CuGaO_2$ with low J_{SC}s resulting. Unfortunately, they did not provide

any comparison devices and given the large semiconductor particles used in this study low J_{SC}s are not unexpected. One surprising system, in contrast to reports of N719 with other p-type semiconductors, is from Shi *et al.* [91] who reported a J_{SC} of 8.35 mA/cm^2 when they applied it to $NiCO_2O_4$. Previously Qin *et al.* [81] saw a very poor response (and no IPCE response attributable to dye sensitisation) from N3 on NiO. Furthermore, in our 2008 paper, a desensitizing response was observed N719, *i.e.*, dyed devices perform worse than undyed [76], which fits in line with the idea that the N719/N3 complex or strongly interact with I^-. This idea was put forward by Clifford *et al.* to account for the fact that this dye is such an effective sensitizer of TiO_2 in nDSCs [112, 113].

In spite of the poor results obtained for N3/N719 on NiO, this is not universally true of Ru based sensitizers. More successful attempts at producing Ru dyes have been reported by Pellegrin *et al.* [107] (with different binding groups, as mentioned above) as well as Freys *et al.* [114], who compared Ru(dicarboxypyridine)$_3$ and Ru(dicarboxypyridine)(4-nitronaphthalene-1,8-dicarboximide) using both I^-/I_3^- and Co(II)/(III) based electrolytes. Here the latter of the dyes contains a strongly electron accepting moiety, having a significant impact on the redox potentials of the dye. In this case the first dye shows a small response with I^-/I_3^-, and almost none with (Co(II)/(III)). The second also shows a modest response when used in a device with I^-/I_3^-, however, an APCE of almost 30% is attained when used in conjunction with a (Co(II)/(III)) electrolyte.

In 2013, Ji *et al. [92]* introduced three dyes (dicarboxylate TPA donor and cyclometalated Ru acceptor). These provided broad absorption and modest J_{SC} values (~2.5-3 mA/cm^2). The following year Wood *et al. [115]* introduced two donor-acceptor type dyes, with similar structures, leading to similar J_{SC}s. Huang *et al.* [116] reported further, similar, sensitizers. However, in the latter example, they employed ITO nanoparticles as the semiconductor. Although this resulted in a photocathodic current, the mechanism for this was not the same as in previous pDSCs. Instead charge generation involves electrons being injected *into the dye from the CB* of the degenerate semiconductor.

One further issue that may limit the applicability of Ru complexes in pDSCs are the relative low extinction coefficients of Ru complexes, leading to low light harvesting efficiencies when used with NiO - parasitic absorption limits the amount of light that can be harvested by the dye, even if the semiconductor layer is made to be thick, as is typically the case in Ru complex employing nDSC devices.

2.2.4 INORGANIC SENSITIZERS

Recently, Sun *et al.* put forward the idea of using polyoxometalates, however, to date, these have not been experimentally tested [117]. Meanwhile inorganic sensitizers, including quantum dots have also been utilised by a handful of researchers to create pDSCs. In the first report of a QD sensitized pDSC, or pQDSC, published in 2009, Rhee *et al.* [118], applied Cu_2S to NiO. The broad and featureless shape of the Cu_2S absorption, along with the broad featureless IPCE response of unsensitized NiO (with I^-/I_3^- based electrolyte) led to some ambiguity as to whether this was truly QD sensitized [119], however, the fact that the measured IPCE response doesn't go to zero at 800 nm (the absorption onset of the QDs is around 1030 nm) suggests this device is indeed Cu_2S sensitized, possibly in addition to I^-/I_3^- generated photocurrent. This component of photocurrent is a feature of all I^-/I_3^- based pDSCs.

Interestingly, this first report used I^-/I_3^-, which is known to be corrosive towards materials including metal sulphides. The majority of reports into pQDSC have, however, used a polysulfide redox mediator, S^{2-}/S_x^{2-}, although (Co(II)/(III)) based electrolytes have also been successfully employed as well [120]. Furthermore, dense NiO layers have been shown to be necessary to minimize the back reaction of this mediator at the FTO interface [119, 121]. CdS and CdSe have been the most popular choices of inorganic sensitizer [119, 120, 122-124],

including a dual sensitizer CdSe + CdS system, which forms an energy cascade [121]. Of the CdS systems, only Mao *et al*. have been able to produce devices with J_{SC} in excess of 1 mA/cm^2. Interestingly, this was achieved using CoO as the semiconductor, rather than NiO. Park *et al.* [125] have also managed to attain J_{SC} > 3 mA/cm^2 using CdSe. Here, a V_{OC} of 490 mV was also observed, leading to an overall PCE of 0.35%.

More recently reports have started to emerge of methylammonium lead halide perovskites (MALH) being used in pDSCs. Tian *et al.* [126] reported an efficiency of 0.16 % while Wang *et al.* [127] were able to achieve up to 0.71% (0.91% at reduced light intensity). These first reports used MALH in a manner analogous to that reported in 2011 by the group of Nam-Gyu Park [128], and brought the material to the attention of the solar cell community. It was, however, the implementation of MALH in a solid state device [129] which resulted in the material becoming of interest to a much wider scientific community. In this second implementation, the substitution of the porous TiO_2 layer for Al_2O_3, an insulator, was shown to produce a functioning (even higher PCE) device - raising questions about whether it could be classified as a DSC or as something else. This definition was challenged further with the advent of planar heterojunction structures [130].

Tian *et al.* [126] also used an n-type fullerene derivative, phenyl-C61-butyric acid methyl ester (PCBM) to create a solid state p-type MALH based device, as have others [131]. As well as this, NiO has been used in planar heterojunction devices [132] and monolithic device architectures [133], where device efficiencies of 1.5%, 9.5% and 11.4% were realised respectively. The decision of where to draw the line of device classification is somewhat arbitrary, and the need to draw a line at all is even debatable. On the one hand, it should be emphasised that while researchers may identify different technologies as competition, they should avoid viewing them as being 'the enemy'. On the other hand, some distinction needs to be drawn in order to complete an analysis such as we endeavour to do in this review.

Photocathodes have also been prepared directly from materials such as Se or PbS and combined with photoanodes to create pnDSCs [134-136], with near additive V_{OC}s in the former, but not so in the latter. PbS does however offer significant absorption into the IR.

2.2.5 RED & NEAR INFRARED SENSITIZERS

In pnDSCs, the two sensitizers should be spectrally complimentary to facilitate similar current generation at each electrode under AM1.5 conditions. The electrode generating the largest portion of the overall voltage should absorb in the blue-green part of the spectrum and will (generally) be the front face, thereby reducing thermalisation losses. One of the features of pnDSCs is the (in principle) ability to illuminate from either side, as long as the red-most sensitizer has an absorption window matching the other sensitizer. This may be achieved through the use of molecular sensitizers with discrete orbital energies.

Efforts to address the red-shifting of dyes for pDSCs have, thus far, been few in number. With high quantum efficiencies attained for blue-green absorbing dyes, and general design rules for pDSCs being better understood, it seems reasonable that this should be a high priority area of pDSC development. So far a handful of groups [75, 87, 88, 94, 110, 137] have produced dyes for pDSCs with substantially red-shifted absorbance. In three cases, squarine has been employed as the electron acceptor. The most successful of these has been Warnan *et al.* who realised a 25% IPCE (λ = 620 nm) with a triad (SQ-PMI-NDI) [87]. Wood *et al.* obtained similar results (3.3 mA/cm^2 and 18% IPCE at 625 nm) [88] using an asymmetric TPA based sensitizer. These researchers followed this work up with P1 derivatives containing bodipy acceptor moieties [98]. With this strategy they have been able to sensitized pDSC to well past 700 nm, with IPCE values in excess of 20%. Previously, Mori *et al.*

[75] and Sumikara *et al.* [137] reported dyes with IPCEs of ~1% and 1.8% for NiO and CuO respectively, with for wavelengths up to 790 nm.

It has often been assumed that the photocathode will be the most suitable choice for sensitisation in the red/infrared part of the spectrum, however, recent developments in redox mediator energy tuning and the application of these in highly efficient pDSCs, suggest that this is not strictly true. At the least, researchers should view this with an open mind and consider the possibility of having a blue-green sensitized photocathode with a red-NIR sensitized photoanode. To this end it is worth making a note on the development of red-NIR dyes for nDSCs. With the exception of N749 (Ru(II) "black dye") the field is characterised by low V_{OC}s for dyes with absorption onsets past ~800 nm. One of the most successful examples is a squarine based dye, B1, with an absorption onset around 800 nm. This provides V_{OC} = 591 mV [138], while most other IR sensitised nDSC have V_{OC} < 500 mV [139-142]. As far as we are aware, there has been little work done combining IR dyes with alternate redox mediators.

2.3. ELECTROLYTE

The electrolyte used in a DSC consists of a redox couple (also referred to as redox shuttle or redox mediator), various additives (discussed in brief below) and a solvent. The main task of this is to regenerate the dye after charge injection. In pDSC this means oxidising a photoreduced dye, followed by transport of the reduced mediator away from the surface. The inverse is true for nDSC and of course both are necessary for pnDSC. The electrolyte is one of the two ways in which the electrodes in pnDSCs are joined, the other being the external circuit.

The challenge is to introduce a redox mediator that shows fast dye regeneration and slow interfacial charge recombination between the reduced/oxidized species present in the electrolyte and the injected charge in the semiconductor. To fulfil these requirements, the redox mediator should have a good solubility and high ionic mobility in the solvent of interest, have a sufficient driving force to regenerate the dye, and have fast electron transfer kinetics and to be able to regenerate at minimal over potential at a catalytic counter electrode in the case of single photoelectrode systems [143]. In addition, low light absorption within the visible spectral region allows better light harvesting by the sensitizer [144].

2.3.1 REDOX COUPLES

As seen previously (Section 1.3), the redox mediator sets one of the limits to the device V_{OC}. Until recently, triiodide/iodide (I_3^-/I^-) has been almost exclusively used and best performing redox shuttle employed in pDSCs (and nDSCs for that matter). Although this redox mediator has been extensively applied and studied within pDSCs, the small difference in potential between I^-/I_3^- (-4.8 eV vs vacuum) and VB edge of NiO (-5.15 eV vs vacuum) limit the reasonably attainable device V_{OC}s [5, 38, 76, 143]. In 2012, Zhang *et al.* reported a device PCE of 0.61% with a V_{OC} of 350 mV, which is both the best reported efficiency and highest V_{OC} achieved with I_3^-/I^- redox mediator, and based on the above values very close to the limit for V_{OC} in this system, [83, 145] as per the discussion in Section 1.3. There are also disagreements regarding the above quoted values of VB edge and redox potentials [146, 147]. Furthermore, the actual redox potential of the couple is dependent upon the relative concentrations of each species in accordance with Nernstian principles, as well as solvent effects (which will be discussed below).

On account of the small offset between the redox potentials of I^-/I_3^- and the VB edge of NiO, there has been a drive to change one or both of these components in order to achieve higher V_{OC} in pDSC devices. There is of course a counter argument to be made against changing the mediator simply to attain higher voltages, based on the fact that the V_{OC} of a pnDSC is not limited by the mediator, but rather ${}_qE_f$ of electrons in the n-type and holes in the p-type semiconductor - in short, what is gained on one side is lost to the other (see Figure 4c). On the other hand, altering the redox potential of the mediator can allow for a greater level of device design flexibility, especially when mediators such as organometallic redox complexes are employed, where the redox potentials can be tuned based on ligand selection [148]. Furthermore, there are a number of other reasons why the I^-/I_3^- mediator should be replaced, besides the small energy offset:

- The corrosive nature of I^-/I_3^- limits applicability in modules as typical current collectors such as silver or copper are readily dissolved by I^-/I_3^-. Furthermore many inorganic sensitizers and plasmonic structures cannot be combined with this mediator.
- Iodine is itself volatile and can sublime if it is not securely encapsulated.
- There is an inherent energy loss as the two electron reduction and oxidation processes process via intermediates [149, 150]. Several authors have shown the ($I_3^-/I_2^{\bullet-}$) potential to be a major impediment to dye regeneration in pDSC [82, 94].
- Polyiodides absorb blue and green light, in competition with sensitizers.
- Photocathodic current generation of polyiodides has a low quantum efficiency and doesn't benefit the photoanode [78, 151-153].

Below (Figure 9) shows the two one electron redox potentials associated with I^-/I_3^-. Here, Gibson *et al.* also show that these potentials can shift dramatically due to solvent effects [149].

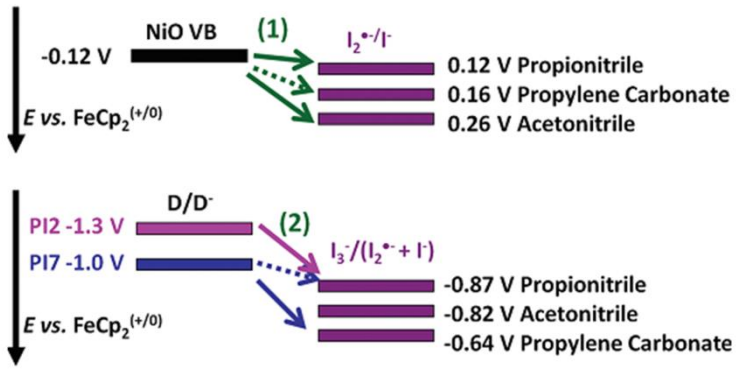

Figure 9 – Recombination reaction (hole transfer from NiO to electrolyte) and dye regeneration for I^-/I_3^- (and specifically the intermediate reactions) in different solvents – Reprinted with permission from Gibson *et al.*, Langmuir 28(15). Copyright 2012 American Chemical Society [149].

Light absorption by polyiodides can result in moderate photocurrents. This has been noted to be at least partially responsible for IPCE features around 380 nm, rather than NiO or the dye [154]. Below (in Figure 10a) it can be high concentrations of I_2 in PC based electrolytes lead to the creation of higher order polyiodides with different absorption spectra, which are also photoactive. Figure 10b demonstrates that this photoactivity of polyiodides exists even in the absence of NiO, however the magnitude is decreased. In nDSCs this mechanism runs counter to the intended photoanodic operation [151].

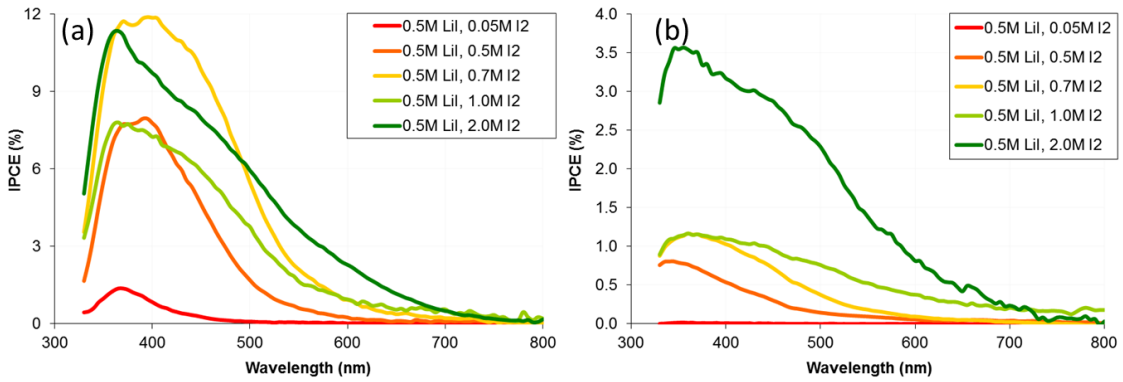

Figure 10 – IPCEs of pDSC with electrolytes containing 0.5M LiI and various concentrations of I_2 with (a) undyed NiO (b) no semiconductor (FTO|electrolyte|Pt|FTO). Modified from [154].

A key challenge for higher efficient p-DSCs is the development of a redox mediator with; (i) a suitable redox potential; (ii) fast electron kinetics for dye regeneration, but sufficiently slow to supress recombination reactions; and (iii) low absorption of visible light. The first reports of alternative redox mediators for pDSC came in 2009 with (Co(II)/(III)) complexes used by Gibson *et al.* [155]. Since this, other cobalt complexes [85], polysulfides [119], iron complexes [84] and thiol/dithiol compounds [66, 156] have been successfully employed, with a selection of these shown below in Table 4, as well as in Figure 11.

Table 4 – redox couples used in pDSC

Compound structure and name	Redox potential (conditions, ref)
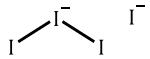 Iodide-triiodide	0.53 eV (vs NHE) ; 0.4M LiI, 0.04M I_2 in Acetonitrile[146]
	0.315 eV (vs NHE); 0.6 M BMII, 0.03M I_2 in acetonitrile:valeronitrile mix [85]
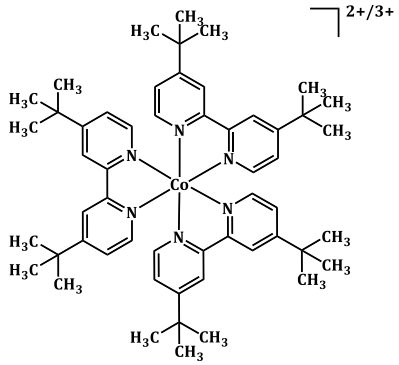 $[Co(dtb\text{-}bpy)_3]^{3+/2+}$(dtb-bpy = 4,4'-di-tert-butyl-2,2'-dipyridyl)	-0.26 eV (vs ferrocene); 0.1M/0.1M Co^{2+}/Co^{3+} in propylene carbonate[64]

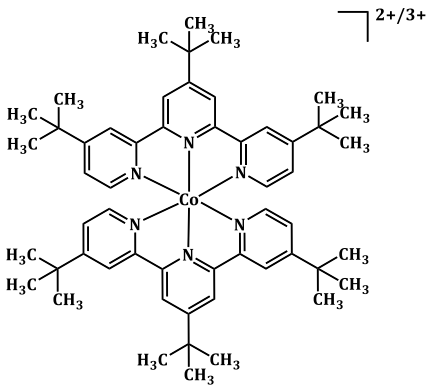

$[Co(ttb\text{-}tpy)_3]^{3+/2+}$ (ttb-bpy = 4,4',4"-tri-tert-butyl-2,2':6',2"-terpyridyl)

-0.32 (vs ferrocene); 0.1M/0.1M Co^{2+}/Co^{3+} in propylene carbonate[64]

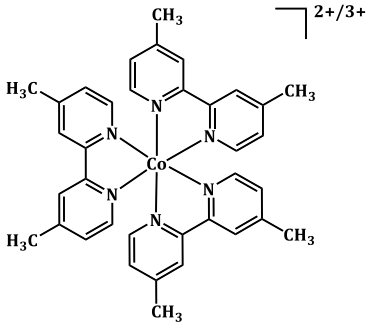

$[Co(dm\text{-}bpy)_3]^{3+/2+}$ (dm-bpy = 4,4'-dimethyl-2,2'-dipyridyl)

-0.23 (vs ferrocene); 0.1M/0.1M Co^{2+}/Co^{3+} in propylene carbonate[64]

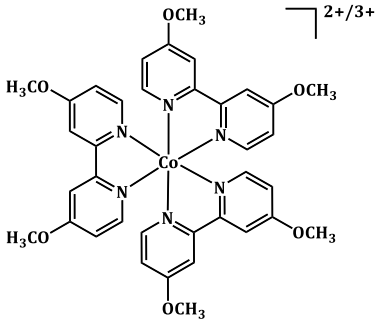

$[Co(dMeO\text{-}bpy)_3]^{3+/2+}$ (dMeO-bpy = 4,4'-dimethoxy-2,2'-dipyridyl)

-0.28 (vs ferrocene); 0.1M/0.1M Co^{2+}/Co^{3+} in acetonitrile[64]

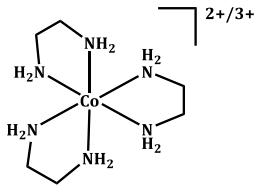

$[Co(en)_3]^{3+/2+}$ (en = ethylenediamine)

-0.25 eV (v NHE); 0.07M $[Co(en)_3](BF_4)_3$, 0.3M $Co(BF_4)_2 \cdot 6H_2O$ in acetonitrile

- 5.51 eV (vacuum scale); 0.3M T^-, 0.9M T2 in 7:3 MeCN:PC[156]

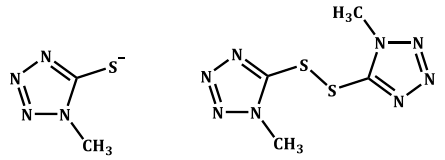

1-methy-1H-tetrazole-5-thiolate monomer and dimer (T^-/T_2)

0.485 (vs NHE); 0.4M T-, 0.4M T2 in acetonitrile and ethylene carbonate mix[157]

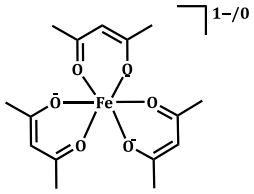

$Fe(acac)_3^{(0/1-)}$ (acac = acetylacetonato)

-0.2V (v NHE); 0.1M $(NBu_4)[Fe(acac)_3]$, 0.05M $[Fe(acac)_3]$ in acetonitrile[84]

The 2009 report of Gibson *et al.* of a pDSC with $[Co(dtb\text{-}bpy)_3]^{3+/2+}$ (dtb-bpy = 4,4'-di-tert-butyl-2,2'-dipyridyl) as the redox mediator [155], in conjunction with the PI-NDI sensitizer (Table 3), it was used to provide a PCE of 0.20% and a V_{OC} of 350 mV. The same group followed this with a study of a series of cobalt(II)/(III) tris(bipyridyl) complexes (Table 4) in 2011, however, none of these redox mediators could surpass an efficiency of 0.25%, which was attributed to interfacial charge recombination reactions [64].

The efficiency of a pDSC using $[Co(en)_3]^{3+/2+}$ (en = ethylenediamine) redox mediator was demonstrated to be much higher [85]. Powar *et al.* achieved a record efficiency of 1.30% with a J_{SC} of 4.44 mA cm^{-2} and a V_{OC} of 709 mV for these devices in conjunction with PMI-6T-TPA (Table 3). The significant improvement was largely due to the substantially higher V_{OC} obtained as a result of the favourable redox potential of −0.03 V *vs.* NHE, compared to the previous (Co(II)/(III)) based mediators. Importantly, the use of $[Co(en)_3]^{3+/2+}$ is seen to be effective for dye regeneration, in spite of this dramatically higher redox potential.

In 2013 and again in 2014, Xu *et al.* [66, 156] employed 1-methy-1H-tetrazole-5-thiolate and the corresponding disulphide dimer (T^-/T_2) as an alternative to I^-/I_3^-. This was particularly relevant for their work with plasmonic nanostructures, made of gold, which could be rapidly corroded by I^-/I_3^-. Although this mediator was reported to have a very low redox potential of -5.51 eV (vacuum scale), this should be read in the context of them measuring I^-/I_3^- at -5.56 eV, in contrast to the bulk of other reports on the potential of this mediator. Moreover, Wang *et al.* have reported T^-/T_2 in nDSCs (attaining 6.4% PCE) with a redox potential of 0.485 eV (vs NHE) [157].

Figure 11 shows a selection of redox mediators used in pDSCs. It is particularly interesting to note the potential range over which cobalt complexes can be tuned through ligand selection.

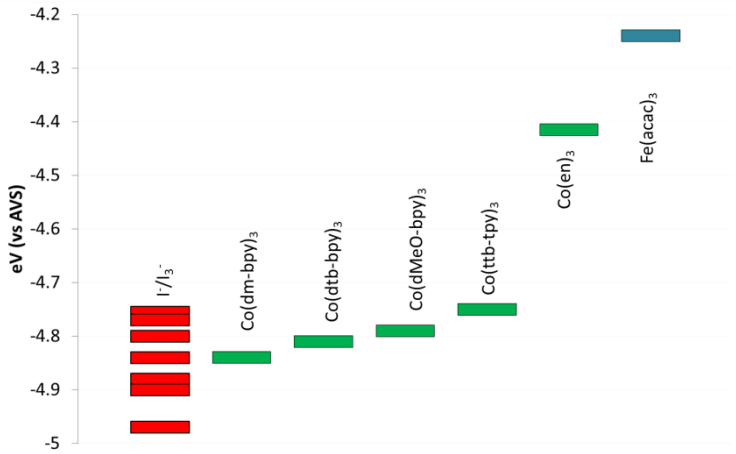

Figure 11 – Reported potentials of redox mediators in pDSC, converted to vacuum scale (at 4.44 eV vs NHE)[158].

Recently, we reported the use of tris(acetylacetonato)iron(II)/(III), $[Fe(acac)_3]^{0/1-}$ as a mediator in pDSC [84]. This one electron mediator has a redox potential of -0.2 V (*vs.* NHE), leading to an even larger difference in potential than was seen for $[Co(en)_3]^{3+/2+}$. Charge recombination was shown to lead to slightly lower V_{OC} than was expected. Application of a nickel oxide (NiO) blocking layer on the working electrode, and chenodeoxycholic acid as a co-adsorbant were required to suppress these unfavourable back reactions at the electrolyte/working electrode interface. In spite of this issue, a J_{SC} of 7.65 mA/cm^2 and PCE of 2.51% were realised. The high diffusion rates afforded this high J_{SC}s and good scaling of performance with light intensity. There exists the possibility of fine tuning the redox potential of these complexes by either varying the metal centre or the acetylacetonate ligand by introducing different groups.

2.3.2 ELECTROLYTE SOLVENT

While the solvent is an often overlooked component of the electrolyte, it plays a significant role in the performance of the device. It provides the medium for dissolution and diffusion of the ionic conductors. The types of solvents in use, and prerequisites for electrolyte solvents, are same for both n- and p-DSCs (and consequently for pnDSCs). A few main requirements for a good solvent are [159-162]:

- Melting point below −20 °C and boiling point over 100 °C to avoid solvent freezing and evaporation respectively, in outdoor applications and to retain long term stability.
- High dielectric constant to ensure complete dissolution of the redox couple and any additives
- Low viscosity that leads to a high diffusion coefficient of the redox mediator that improves the conductivity
- Low light absorption in the visible and NIR regions
- Inert towards metal contacts
- Low toxicity
- Low cost

A large number of organic solvents, such as esters, lactones, alcohols, tetrahydrofuran, and *N*,*N*-dimethylformamide have been utilized in DSCs [21, 163, 164]. Moreover, a variety of nitriles such as acetonitrile, methoxyacetonitrile, 3-methoxypropionitrile, valeronitrile, and glutaronitrile have also been studied [161]. Among them, acetonitrile is the most widely used solvent for electrolytes due to the high solubility of salt components of the electrolyte, low viscosity, and excellent chemical stability, especially in the laboratory, where

it allows for construction of devices without mass transport limitations, leading to high efficiencies. To date, the highest pDSC PCE (2.51%) was achieved with an acetonitrile based electrolyte [84]. On the other hand, the low boiling point of ~82 °C (and high vapour pressure) along with relatively high toxicity, limit its large scale application. Therefore, mixtures of nitriles are often used to reduce solvent volatility [162]. Another extensively studied nitrile is 3-methoxypropionitrile, which has a melting point of -63 °C and a boiling point of 164 °C. Due to its good chemical stability and low toxicity compared to acetonitrile, it has become a common solvent used in DSC electrolytes nowadays. Devices based on 3-methoxypropionitrile were found to retain 98% of their initial efficiency after 1000 h at 80 °C when kept in the dark. Also, the performance degradation was reported to be negligible after 1000 h of visible light soaking at 60 °C [162, 163, 165].

It needs to be appreciated that the solvent affects the redox potential of not only the mediator (see Figure 9 above), but also the dye and the semiconductor. Many early reports of pDSC devices have utilised propylene carbonate, possibly due to the resulting increase in driving forces for charge regeneration [149]. This requirement does not seem to apply with many of the more recent, donor-acceptor, dyes. This is of substantial benefit to tandem devices as propylene carbonate, being a protic solvent, has a significant effect on the CB edge potential of TiO_2, leading to lower overall V_{OC}s.

One method to circumvent the issues related to solvents is to employ a solid state architecture, such as the MALH devices mentioned above (Section 2.2). A dye-sensitized example has been reported by Zhang *et al.* with P1 sensitized NiO using PCBM and an aluminium top contact [166]. To date we are not aware of any solid state pnDSCs, and indeed it would most likely require resolution of quite a number of technical issues in order to produce such a device.

2.3.3 ELECTROLYTE ADDITIVES

One more concern for the creation of an electrolyte suitable for the use with both photoanodes and photocathodes is the inclusion of various electrolyte additives. These have been utilized in nDSCs to enhance the device performance by mitigating recombination processes and / or altering the density of states of the semiconductor. To date there has been little evidence to suggest analogous effects in pDSC. Nitrogen containing heterocyclic compounds have been applied in nDSCs since 1993 [164], with the most commonly used compound being *tert*-butylpyridine (tBP). A number of authors have reported that tBP reduces the charge recombination reactions at the electrolyte/TiO_2 interface [167-171]. The absence of any effect on the photocathode is not necessarily an issue; in the design of complex structures, such as tandem devices the ability to optimize one electrode without significant effect on the other maybe viewed beneficially.

2.4. p-TYPE SEMICONDUCTORS

In p-type semiconductor materials, the density of holes is greater than that of free electrons. As such the majority charge carriers are holes and as a result, the E_F of these materials lies closer to the VB than the CB. As a critical part of the pDSC architecture, there have been review articles focussing solely on different NiO structures [36] and p-type copper delafossite materials for pDSC [30].

2.4.1 NiO

Nickel oxide, NiO, has been the most widely used semiconductor material in p-DSCs. Nevertheless, there are drawbacks associated with NiO. By being a strongly coloured material NiO typically absorbs 30-40% of incident light in pDSCs and, therefore, limits the device performance significantly [28].

Extensive studies on NiO have shown that it is a wide band gap material (3.6-4.0 eV) with a high charge carrier density. Mesoporous NiO photocathodes have been deposited using a variety of methods, such as nanocasting [145], electrodeposition [172], hydrothermal synthesis [74, 173], spray pyrolysis [119, 174], sol-gel synthesis [5, 175], doctor blading [76] and screen printing [28, 85, 176]. The latter two of these strategies allows for the use of a range of particles, which may be difficult to produce *in-situ* [83, 176]. In addition to these strategies, some authors have also explored options such as anodisation of nickel metal structures [177].

J_{SC} values generated within the device have been improved by using materials specifically engineered for purpose, such as NiO microballs (composed of many smaller nanoparticles) [176]. The high surface area, good electrical connectivity and favourable pore size distribution of these microballs, even after sintering, facilitated higher dye loading than nanoparticles, lessening parasitic absorption, resulting in better light harvesting efficiencies [176].

Two papers by Zhang *et al.* highlighted the importance of highly crystalline structures in NiO based pDSC [83, 145], with substantial increases in charge carrier lifetime resulting. This may be seen to be related to surface state mediated recombination mechanisms, as per the discussion introduced by Smeigh *et al.* [178], where they see evidence of a Marcus normal relationship (as opposed to TiO_2 systems which show inverse Marcus behaviour) between the driving force and the rate of recombination of the dye anion and the hole in NiO. Here defects in NiO (specifically trap states) play a major role. This of course runs counter to the need for a large ΔG_{reg}, as observed by others.

Charge transport in NiO was also probed by D'Amario *et al.* [179], specifically in response to the question of whether NiO was capable of supporting high (comparable to the best nDSCs) current densities. They found high conductivity in mesoporous NiO, in spite of comparatively low values in the bulk. Additionally, they observed the effects of Li doping, resulting in a VB edge shift, leading to a higher device V_{OC}. In a similar way, several authors have investigated doping of NiO with various metals, including Li [180] Co [181], Mg [182]. Shi *et al.* [91] employed the ternary oxide, $NiCo_2O_4$, in order to realize very impressive results (V_{OC} = 189 mV, J_{SC} = 8.35 mA/cm^2, PCE = 0.785 %). Incredibly, this was achieved using N719 and I^-/I_3^- as the dye and redox mediator respectively.

In all these cases, the high surface area (as required to facilitate high dye loadings and hence high light harvesting efficiencies) also leads to capacitive behaviour. It is therefore critical that researchers ensure their current-voltage measurements are conducted correctly, ensuring minimal influence of these artefacts. Below, in Figure 12a, four devices, with varying NiO thicknesses, and therefore total surface area, were measured in the dark at different sweep rates [154]. The apparent dark J_{SC} highlights the magnitude of possible measurement errors (overestimation) if the voltage sweep is completed too fast. Figure 12b shows the response a device produced by Powar *et al.* [85], using a (Co(II)/(III)) electrolyte, which is seen to provide have a different efficiency based on the sweep rate and direction. Here, capacitive effects are coupled with diffusion limitations of the mediator.

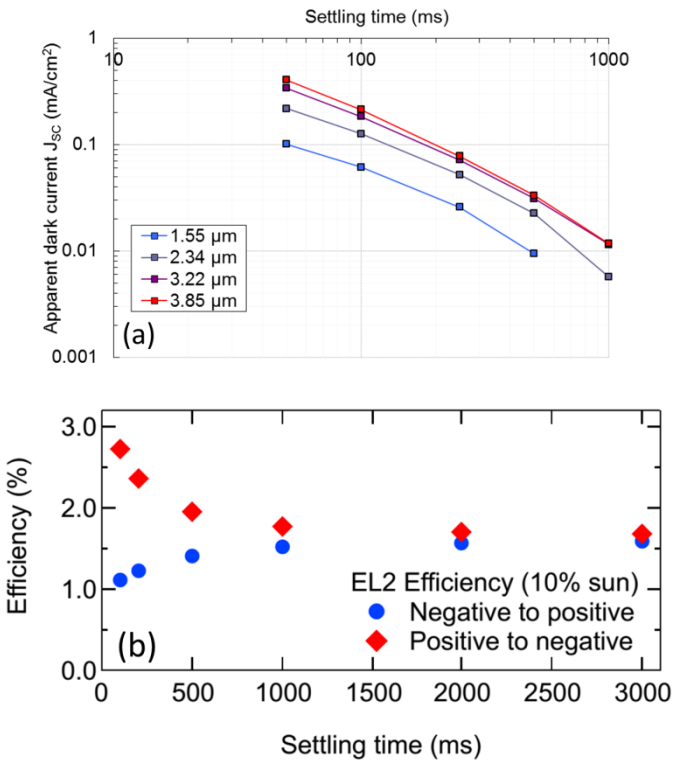

Figure 12 – (a) apparent dark current as a function of settling time for various thicknesses of NiO film, step size = 10 mV (from [154]) (b) Measured efficiencies of pDSC devices with forward and reverse sweeps with different settling times (10 mV step size), Image reproduced from Powar *et al.*, Angewandte 52(2), copyright 2013 [85].

2.4.2 OTHER p-TYPE SEMICONDUCTORS

Due to the closeness of the redox potential of the commonly used I_3^-/I^- based electrolyte and the VB edge of NiO, the attainable V_{OC}s are limited (with the typical estimation being around 0.35 V) [28]. Therefore, researchers investigated alternative p-type semiconductors with a more positive VB edge. CuO [137], $CuAlO_2$ [183], $CuCrO_2$ [65, 184], and $CuGaO_2$ [185] are some materials that have been tested in p-DSCs to overcome this problem. Even though larger V_{OC}'s have been achieved with these materials, the J_{SC} has always been lower than those of the devices based on NiO, often due to the smaller surface area, which determines the amount of dye adsorbed (see Figure 13 below as an example of this).

Although V_{OC} can be also be increased by a more judicious choice of redox mediator, it is imperative that researchers also find p-type semiconductors to replace NiO. When used with TiO_2, the attainable V_{OC} of a pnDSC remains low. Indeed single junction nDSCs can surpass the V_{OC}s of the best pnDSCs to date [186].

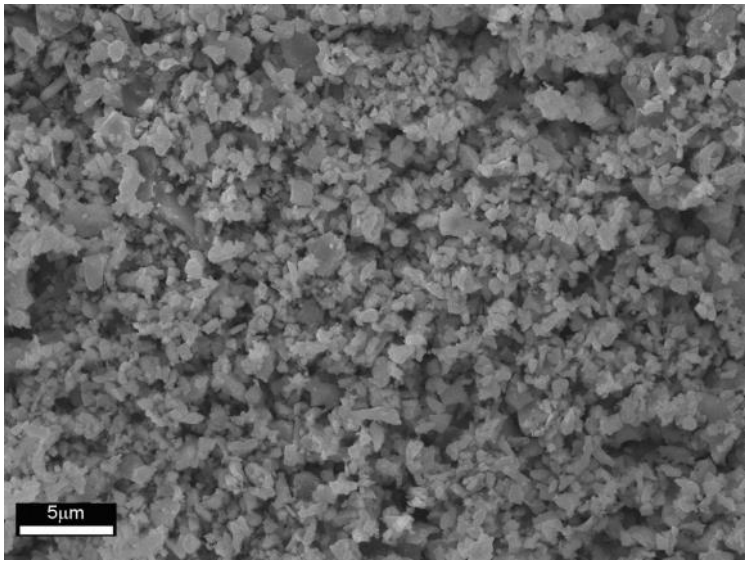

Figure 13 – SEM image of $CuAlO_2$ surface, demonstrating large particle sizes which lead to low dye loading and account for the low J_{SC} values observed (from Nattestad *et al*. [183]).

Many of the most studied alternatives to NiO are Cu based delafossite materials [30], and are particularly interesting as they have slightly depressed VB edge energies compared to that of NiO. This also allows for many of the proven dyes for pDSC (shown on NiO) to also be used here. Looking forward, with larger changes in the VB edge, this will obviously need to be addressed with the creation of new dyes. The VB edges of these materials has been shown to be defined by the Cu 3d band (~ -5.1 eV AVS), with the other metal species serving to slightly mediate this. Below in Figure 14 is a selection of reported values for band edge potentials of p-type materials. As with dyes and redox mediators, there are some discrepancies over exact values. This may arise from experimental condition or even conversion factors [158].

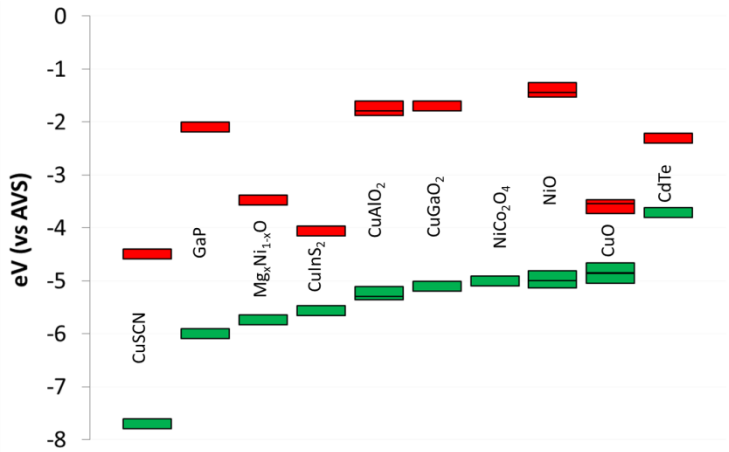

Figure 14 – VB and CB edge potentials of selected p-type semiconductors (values obtained from various reports [5, 15, 18, 23, 80, 91, 125, 137, 187-190], note, CB edge potential of $NiCo_2O_4$ was not reported).

2.4.3 CORE-SHELL STRUCTURED PHOTOCATHODES

The problem of charge recombination has been tackled in a number of ways in nDSCs. Hihgly faceted crystals, organic shielding agents (such as phosphinic acid [191]) and sensitizers with surface shielding groups [192]. have been employed to inhibit contact between the electrolyte and the semiconductor, while other

researchers produced core-shell structured electrodes to tackle this issue [193]. In pDSC, the problem of recombination has been recognised as substantial since the early reports [38]. The most successful approach to date for reducing recombination has been the use of donor-acceptor sensitizers (as well as the use of highly crystalline materials with lower defect concentrations [83, 145]), however core-shell structures have also been employed. Here a thin concentric layer of a second material is applied to the semiconductor film prior to sensitisation. Although a cascade configuration may be used [194], typically an insulating material is used, where this shell means that charge transfer (in both directions) is impeded and can only occur by tunnelling, as there is no direct electronic pathway from the dye to the semiconductor. Schematics of core-shell structured photoelectrodes are shown in Figure 15.

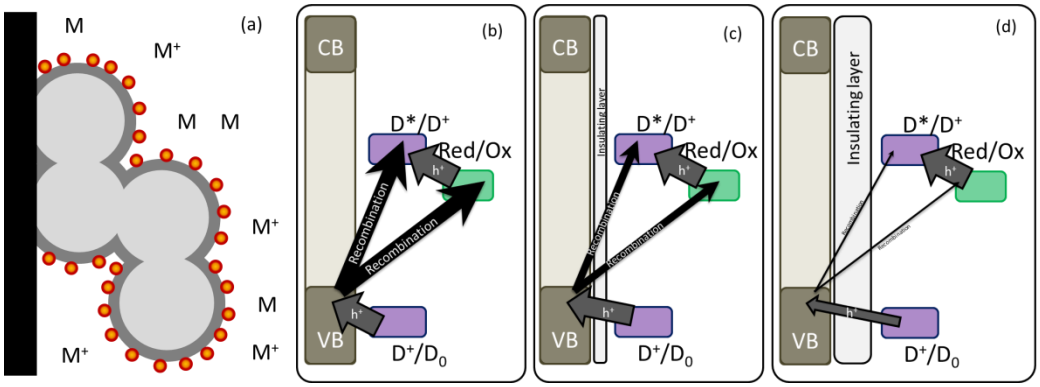

Figure 15 – (a) Schematic representation of a core-shell structured film (M, M^+ represents the mediator in reduced and oxides forms respectively). The core material (light grey) is isolated from the electrolyte and the dye molecules by a shell material (dark grey). (b-d) Schematic of the effects of core-shell structuring (and shell thickness) on rates of charge injection and recombination.

This insulating layer results in an asymmetric decrease in the rates of charge injection and recombination (see Equation 1 and Figure 15b-d). Typically, if the shell material is more than a few nanometers thick charge injection is decreased to a point where overall performance suffers dramatically (as seen schematically in Figure 15d). Dye injection occurs on the scale of fs to ps [37] whereas the recombination path occurs in the range of µs to ms [28, 39].

$$\phi_{inj} = \frac{k_{inj}}{k_{IC} + k_{inj} + k_{fl}}$$

And

$$\phi_{reg} = \frac{k_{reg}}{k_{reg} + k_{recom}}$$

φ_{inj} = probability of injection
φ_{reg} = probability of dye regeneration
k_{inj} = injection rate
k_{IC} = internal conversion rate
k_{fl} = fluorescence rate
k_{reg} = regeneration rate
k_{recom} = recombination rate

Equation 1 – Charge injection and regeneration probabilities.

Where a tunnelling barrier exists, the rates of k_{inj} and k_{recom} both decrease. For a thin barrier, this has minimal effect on φ_{inj}, as the time constant k_{inj} is the dominant value and exists in both the top and bottom of this equation, essentially cancelling itself out, unless the barrier is large enough to decrease this time constant by several orders of magnitude. Φ_{reg} is improved by the decrease in the k_{recomb} value.

Core-shell structured NiO electrodes were employed by both Natu *et al.* and Uehara *et al.* with modest improvements to device efficiency [40, 41]. To the best of our knowledge these are the only two examples to date, and both employ Al_2O_3 as an insulating shell. Both saw small increases in J_{SC} and more substantial improvements in V_{OC} resulting from the use of this configuration. Natu *et al.*, also saw that the V_{OC} continued to increase with thicker layer, but the J_{SC} was negatively impacted, presumably as charge injection was significantly impeded by the insulating layer.

2.5. SYSTEMS RELATED TO pDSC

The literature also contains a number of systems which bear similarity to pDSC, with similar modes of operation and / or functionality to pDSC systems. Some of these are inspired by, while others can be seen to have helped inspire pDSC. In this section we highlight a couple of these, with specific interest to (i) lessons that can be learned for pDSC development and (ii) ways in which pDSC research can be translated other fields to broaden its impact. The list below is of reports which may be of interest to researchers in this field, however do not strictly fall into the category or pDSC or pnDSC:

- Sensitized GaP was first reported by Memming [16], and served as an important study in determining the nature of p-type sensitisation. This system continues to be the subject of investigation [195]. Similarly, CuSCN was the subject of early p-type sensitisation studies [18, 19].
- CuSCN has also been used as an inorganic hole transport material in nDSCs [22].
- Nakabayashi *et al.* [196] reported photocathodic currents resulting from the sensitisation of p-doped diamond structures using $[Ru(bpy)_3]^{2+}$.
- In 2010 Takechi *et al.* [197] reported the use of a tetrathiolporphyrin-bithiophene photocathode. With a platinum counter electrode, they were able to achieve V_{OC} = 290 mV, J_{SC} = 0.45 mA/cm^2 for a total PCE of 0.05 % (with 5 % IPCE @ 420 nm). Combined with a N749 stained TiO_2 photoanode they observed V_{OC} = 970 mV, J_{SC} = 2.3 mA/cm^2 providing a PCE = 0.51 %. Again this device produced an 'S' shaped current-voltage curve, similar to seen in Figure 3.
- Splan *et al.* [198] inadvertently produced a photocathodic device after multilayer dye sensitisation. Here they measured cathodic photocurrent with the dye bound to the ITO substrate and photocathodic with TiO_2. This appears to be the similar to the mechanism proposed by Huang *et al.* [116].
- Matsuda *et al.* [151] also realised the creation of a pDSC unintentionally, as the result of using of very high I_2 concentrations in their electrolyte, *i.e.* polyiodide sensitisation.
- NiO has been used in organic photovoltaic devices (OPV) and planar heterojunction 'perovskite' devices as a hole transport material [199, 200].

2.5.1 MALH (PEROVSKITES)

In Section 2.2, we briefly discussed the application of MALH as a sensitizer in pDSCs [126, 131], as well as the impact this material (or more correctly class of materials) is having to PV research [129]. The intersection between this class of materials and pDSC should not be underestimated. A review of this area from Li *et al.* [201] shows remarkable progress in perovskite production through the use of NiO, the staple of pDSC. A key point is that inorganic materials, such as NiO, CuI and CuSCN, offer a greater chemical stability as compared to organic hole transport materials.

As MALH is the most critical material (and the only light harvester) in these devices it is arguable that the role of NiO (or other p-type material) is more akin to how O'Regan [22] and others [27] have utilised the materials in DSCs, i.e.,. the Dye-Sensitised Heterostructure mentioned in Section 1.2. The reader's attention is drawn back to the discussion surrounding definitions of categories in Section 2.2. Nevertheless, tandem designs incorporating MALH perovskite materials would be a very interesting development. It also seems highly probable that this area of research would be strongly informed by developments in pnDSC.

2.5.2 SENSITIZED PHOTOCATHODES FOR WATER SPLITTING

As with nDSC, there is a great deal of knowledge, acquired from years of development, which can be translated to other technologies. One of the most obvious is water splitting. In 2012, Li *et al.* reported the use of their P1 sensitizer on NiO for water reduction to generate H_2 gas [202]. This was accomplished with the aid of a cobalt co-catalyst and triethanolamine as a sacrificial electron donor. Later the same year, Tong *et al.* reported the first adaptation of a photocathode from pDSC to water splitting without the need for either this sacrificial material or secondary catalyst [203]. This system used the dye PMI-6T-TPA, which remained strongly bound to NiO after extended time periods on account of its hydrophobicity resulting from hexyl chains that prevented water from reaching the semiconductor surface where they could attack the carboxylic linkers. Tong *et al.* combined this dye-sensitized system with $BiVO_4$ to complete total water splitting by solar illumination. More recently Li *et al.* [204] have revisited their aforementioned system, binding the secondary cobalt co-catalyst to the NiO surface and combining with an analogous n-type system (small molecule organic dye and Ru catalyst both bound to TiO_2). In 2014, Park *et al.* reported CdSe sensitized NiO for hydrogen reduction [125], as well as in a pDSC device [124].

To date all these photocathodic systems are only capable to produce current densities in the $\mu A/cm^2$ range, making them the limiting step again (with the best photoanodes producing O_2 at much rate). It is hoped that with continued improvement to photocathodes for pDSCs further improvements will be realised here. Additionally, it is important to understand why sensitizer-semiconductor systems capable of producing modest current densities (> 5 mA/cm^2) in pDSC devices cannot be directly translated to these systems.

2.6 META ANALYSIS OF pDSC DEVELOPMENT

Rightly or wrongly, device efficiency is often the primary metric with which people will judge a device, and is arguably one of the major reasons for the slow initial uptake of research in the field of pDSC. On the other hand, meta-analysis of reported pDSC efficiencies *does* provide an interesting picture and suggests the prospects for this technology may be more promising than some might believe. Below, in Figure 16a, are the reported PCEs from 103 reports of pDSC devices (from which nearly 250 devices were identified). The trend here is obviously impressive, with more than a 350-fold increase in reported efficiencies, realised in an approximately exponential fashion (see grey shaded area in Figure 16a, with red data points representing record PCEs). For this analysis, solid state MALH devices have been excluded. Green data points have been included to show development in record nDSC devices for contrast.

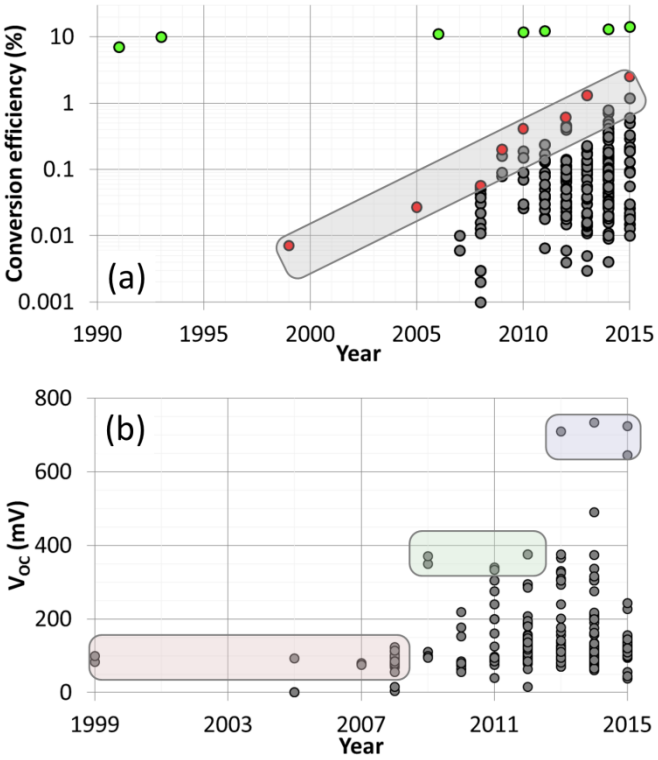

Figure 16 - (a) pDSC device efficiencies, with champion cells in red and champion nDSCs in green for comparative purposed and (b) V_{OC} of pDSC devices.

The above trends illustrate rapid development in this field, with the PCE of champion cells increasing rapidly and in an apparent exponential manner since the first report in 1999 [5]. While this trend is impressive, it is of course not possible that this trend can continue indefinitely; however, it can be hoped that this will at least continue long enough to realise pDSC with comparable efficiencies to champion nDSCs (as will be required for truly high efficiency tandem devices). Modelling in this way does serve to illustrate the rapid rate of improvement which can be attained when device development is tackled on several fronts by researchers from a wide range of academic backgrounds, leading to dynamic research. It should also not be ignored that the field has benefited immensely from developments in nDSC (even where these developments didn't translate to record nDSC efficiencies).

Analysis of the evolution of pDSC V_{OC} values reveals a 'punctuated equilibrium' (Figure 16b). From the initial report of the pDSC, with a V_{OC} of 80 mV, the first major step improvement was realised 2010-2011. Interestingly, this is that this came about on three fronts simultaneously:

1. Reduced recombination (and possible dipole effects) leading to NiO-I^-/I_3^- systems producing higher V_{OC}s [28].
2. The use of alternate redox couples such as (Co(II)/(III)) complexes [64].
3. Introduction of $CuMO_2$ semiconductors with lower lying VB [65, 183, 205].

The second big step was realised with a new generation of redox mediators even better suited to pDSC, with device V_{OC} values are close to those obtained by nDSC [84, 85]. In both nDSC and pDSC, the loss in potential (with most sensitisers having an absorption onset in the rage of 1.5 - 1.8 eV) continues to present a major impediment towards the realisation of competitive DSC PCEs.

A table of the above data can be found in the appendix along with notes on the nature of the development reported in each article. This rapid development suggests that further improvements should be achievable and

there is a strong likelihood of pDSCs being able to attain similar PCEs to nDSCs in the near future. This of course would have major repercussions for pnDSC efficiencies.

3. THE FUTURE OF pDSC RESEARCH

3.1. CHALLENGES for pnDSC AND pDSC

Obviously a number of challenges still exist, limiting the realisation of truly high efficiency pnDSCs. While the bulk of these specifically relate to development of the photocathode, there are still challenges to be met with further development of the photoanode. Two of these are the creation and implementation of high performance red-IR dyes and the search for alternate semiconductors to facilitate higher voltages (either p-type with lower lying VB or n-type with higher CB edge) in pnDSCs.

The creation of red-NIR sensitized nDSCs has recently become more interesting with pDSCs produced displaying V_{OC}s comparable to those in nDSCs. The second task of replacing the semiconductor material, while not exclusive of the first, does tend to head in the opposite direction. Replacing TiO_2 with a material possessing a higher CB edge potential (vacuum) would have in principle the same effect as replacing NiO with a material of lower VB edge potential. While pushing the CB edge potential up has been a focus of nDSC development, success stories tend to be few and far between [206, 207]. The sections below address the major challenges faced in the mission to create high performance photocathodes for pDSCs, pnDSCs as well as photocatalytic water splitting devices.

3.1.1 PARASITIC LIGHT HARVESTING

As has been discussed both here and elsewhere [208, 209], one of the major limitations of using NiO is its strong colouration. This is the chief limitation in the realisation of higher IPCE values [28, 176] and another major reason, along with VB edge potential, why researchers have investigated a range of alternative p-type semiconductors. Renaud *et al.* [209] claimed this colouration to be largely due to the presence of Ni^0. In order to completely oxidize this material to Ni^{2+}, 900 °C had to be reached. In our previous studies [76] and again in this research, it was seen that the decrease in surface area associated with high temperature processing leads to significantly lower light harvesting efficiency and hence low J_{SC} values.

A number of $CuMO_2$ (M=Al, Ga *etc.*) delafossite materials have been used as p-type transparent conducting oxide materials [210, 211]. This combination of high conductivity and low absorption means they are a promising class of materials for incorporation into photocathodes. The literature shows that there are actually very few wide E_G oxide semiconductors with VB edge potentials in the range of -5 to -6 eV (vacuum scale) [190]. The importance of this range is demonstrated below in Section 3.2. There are several ways around this limitation, including the use of doped and ternary metal oxides, as well as non-oxide p-type materials. Materials such as GaP [16, 195] may again be considered for use. B-doped diamond has also been used in p-type PEC, however the VB edge is around between -4.6 eV [212] and -5 eV [196] against vacuum, making it less than ideal as a replacement for NiO (-5.1 eV).

3.1.2 RED-SHIFTING DYE ABSORPTION

In order to realize high device efficiency, the two electrodes in a pnDSC must have complimentary absorption ranges. In the limited number of examples of pnDSC which have been reported to date, this has not been achieved [5, 28, 29, 98]. The major impediment to this is of course the lack of a high performance red-NIR absorbing photocathode. Alternately, recent developments with (Co(II)/(III)) and then Fe(II)/(III) based mediators have resulted in the creation of pDSC with high V_{OC}s. It is equally valid to look at the development of red-shifted dyes for nDSC. Again, dye regeneration may be an issue, based on the reported electrochemistry of such sensitizers [142, 150]. One of the chief reasons put forward for the poor performance of these red-shifted dyes has been the lower ΔG_{reg} for dyes with stabilised LUMO energy levels. The energy losses associated with intermediates in the I^-/I_3^- system ($I_2^{\bullet-}$) is a contributing factor here. It is hoped that with single electron redox processes, this may be able to be overcome.

Beyond this, it should also be noted that as the VB edge of the p-type semiconductor is lowered or the CB edge potential of the n-type semiconductor is increased (or both), there will be new challenges for dye design, with more stabilised HOMO and / or destabilised LUMO energies required, in order to sensitize these alternate materials.

3.1.3 ELECTROLYTE OPTIMISATION

The I^-/I_3^- couple suffers from being a two electron redox processes, with intermediate processes resulting in substantial energy losses. It also has a strong absorbance throughout the blue part of the spectrum which results in a small (low IQE) cathodic photocurrent [151], which not great for pDSC (low QE) and counter-productive for nDSC. While there is obviously a strong case against using I^-/I_3^- in pDSC and pnDSC (and for nDSC), it has remained the staple as it has lower environmental sensitivity than many of the alternative options [84]. This remains one of the biggest limitations, along with diffusion rates. Bulky (Co(II)/(III)) compounds have been shown to suffer from slow diffusion, limiting attainable current densities, especially at higher illumination intensities [64, 84, 85]. As a result, single electron, small, redox mediators such as (Co(II)/(III)) or Fe(II)/(III) complexes are attractive options. $[Fe(acac)_3]^{0/+}$ has been shown to have diffusion rates near the theoretical limit across a broad range of concentrations [84]. Furthermore, new mediators open up more possibilities for the creation of new photoanodes which may be able to compliment efficient photocathodes. The development and tuning of organic mediators will also be of great interest in this regard.

3.1.4 DECREASING RECOMBINATION / INCREASING THE FILL FACTOR

The issue of charge recombination has, rightly, been a major focus of the development of pDSCs. In an early report, Borgström *et al.* [37] identified rapid recombination between the photoreduced dye and the injected hole in NiO as a major loss channel. This issue of dye-semiconductor recombination spurred researchers to look at creating dyes which would limit this process [80]. Core-shell structures have also employed, albeit with limited success [40, 41]. On a somewhat more positive note, an investigation by Smeigh *et al.* [178] showed trap states in NiO to lead to Marcus normal recombination behaviour, as opposed to what is observed in TiO_2 based nDSCs. This suggests that as ΔG_{reg} is reduced, so should be the driving force for recombination between the dye anion and the injected hole, furthermore, D'Amario *et al.* recently demonstrated deep traps in NiO [179]. In spite of this and low conductivity in bulk NiO, mesoporous NiO appears to be capable of supporting high photocurrents (in the range of 20 mA/cm^2, which is what would be required of a high performance pnDSC.

The modelling of J-V responses by Huang *et al.* [213] examined the effects of resistive and recombinative losses. By recalculating the obtained J-V curve without series resistance, a slight improvement in J_{SC} was seen, while the effects of eliminating photoinduced recombination were shown to have a much more substantial impact. They demonstrated a light dependent recombination mechanism, seen through decreased recombination resistance in electrochemical impedance spectroscopy.

More recently, an extensive investigation published by Daeneke *et al.* [208] identified several other limitations in addition to the issues raised above. The first of these was the electrochromic nature of NiO, which leads to reduced light harvesting efficiencies at biases approaching open circuit (~6% decrease leading to a 3% drop in FF versus a model with this effect removed). They also observed small losses relating to recombination of injected holes with the oxidised species in the electrolyte (in line with the conclusions reached by Huang *et al.*). More importantly, charge injection efficiency was shown to be strongly voltage dependent, based on transient absorption experiments measured at a range of applied biases. In addition to this, the recombination efficiency was shown to also have an applied voltage dependence. It is also important to keep in mind the systems used by researchers to make these analyses. While Huang *et al.* used a small dye, "O2" and I^-/I_3^-, Daeneke *et al.* used PMI-6T-TPA and a $[Co(en)_3]^{2+/3+}$ based electrolyte. In either case, the common conclusions reached indicate the continued need for materials development of almost every component the pDSC architecture.

From the above analyses, it can be seen that there is no fundamental limitation to restrict pDSCs from attaining similar PCEs to nDSCs. Huang *et al.* showed that, if the recombination mechanism can be mediated a fill factor of around 0.6 should be attainable. This is close to what has been predicted [214] to be the limiting value (under 1 sun illumination and at room temperature) for a device operating with a V_{OC} of ~160 mV. This issue should also be viewed in the light that our previous work with current matched photoelectrodes resulted in $FF_{pn} > FF_n, FF_p$ [28], suggesting that the fill factor in a tandem device is again a more complex issue.

3.1.5 DEVICE STABILITY

To date there has been little explicit focus on stability of pDSCs. This is most likely due to an assumption that the challenges are general DSC and not specific. Further to this, the challenges of attaining large currents (high quantum efficiencies) and large device voltages appear to have taken precedence. In order to realise practical devices, it will be necessary to replace the volatile solvents presently in use, as well as any materials which are highly sensitive to atmospheric conditions. This is because encapsulation is never perfect and the more thorough it is, the more it adds to device costs and subtracts from practicality (*e.g.* flexible devices). Solid state nDSCs are often put forward as a way around many of these issues. To date there is one example of this being translated to a pDSC [166].

3.2. MODELLING THEORETICAL EFFICIENCIES

There is a degree of uncertainty regarding how to best determine the limiting efficiency for DSC systems. While Fingerhut [45] presented the case of PEC limiting efficiency and Tayebjee [46] for molecular absorbers, with each applying different assumptions, they reach similar final limiting values for single junction devices (26.8 and 28.9%, respectively), which are both slightly lower than what is predicted by the SQ limit. Dye sensitized systems will almost certainly require a distinct model. On one hand, radiative recombination may be less of a concern as charges are rapidly injected into the CB / VB of a wide E_G semiconductor. On the other hand, energy

offsets are required for this efficient charge transfer without substantial back transfer also limiting performance. As far as we can see, there is no 'hard and fast' rule as to the magnitude of this required energy.

Obviously any modelled system is based on a number of assumptions. Most of these stem from the fact that DSCs operate by a different mechanism to pn junction photovoltaics. As such calculations of their theoretical limits should be re-evaluated. Detailed balance analysis (*eg.* SQ) shows radiative recombination to be a significant loss mechanism under ambient conditions. While it is neglected in this analysis, obviously it will play a role in reality, as shown by Daeneke *et al.* [208] under applied bias. Radiative recombination in wide bandgap materials (such as TiO_2, NiO) is expected to be small compared to what would be expected from the absorber material.

Below (Figure 17a) the AM1.5 spectrum [43] is displayed, punctuated at three wavelengths, λ_1 λ_2 and λ_3, providing two complimentary absorption ranges. Ideally one of these would be adsorbed by a photoanode and the other, the photocathode in a pnDSC. As mentioned, the electrodes are configured such that the device will be limited by the weaker (lowest current density) of the two, meaning that each region should be designed to generate the same photocurrent as the other. In this exercise, we simplify the situation to have very sharp absorption onsets, no parasitic light harvesting from electrolytes, semiconductors or even conductive substrates. In reality these will play a role, but there does not seem to be a *fundamental* reason why the impacts of such materials cannot be reduced to negligible levels.

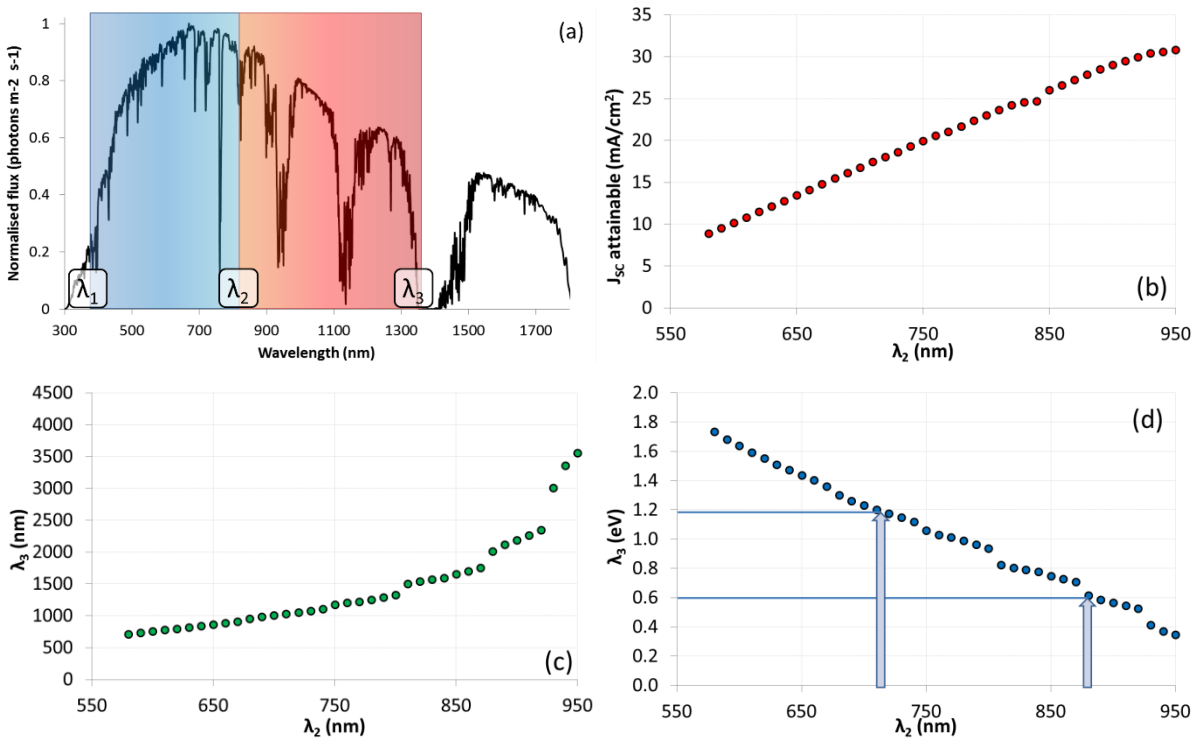

Figure 17 – (a) AM1.5 spectrum with two highlighted regions corresponding to equal photon fluxes, and (b) the upper limit of current density which can be achieved under AM1.5 conditions by harvesting light from 400 nm up to λ_2. (c) The corresponding required wavelength of absorption onset for λ_3 for equal photo flux as between λ_1 and λ_2 and (d) as per (c) in eV.

Figure 17b shows the attainable current density based on light harvested between λ_1 and λ_2. At this point both Φ_{inj} and Φ_{cc} are assumed to be unity, as well as LHE within this band. For this, λ_1 has been set to 400 nm to exclude UV light which is typically damaging to organic sensitizers. This portion of the spectrum can only be expected to generate at most ~0.7 mA/cm^2. If λ_2 exceeds 950 nm, it is actually not possible to harvest enough

photons from the AM1.5 spectrum to current match, as can be seen in figure 17c, which plots the value of λ_3 required to meet the demands of the other electrode harvesting between λ_1 and λ_2. Figure 17d replots this with λ_3 as photon energy. The two highlighted λ_2 values here are of interest as they correspond with the requirement for λ_3 to be (i) 1.13 eV (1100 nm) and (ii) 0.6 eV (2066 nm). These two values are highlighted as: (i) to date the most red-shifted dyes to show at least moderate photoresponses in nDSCs are Os(II) compounds, with onsets around 1100 nm [215, 216]; while (ii) a dye with absorption onset of 0.6 eV would provide no additional voltage if ΔG_{inj} and ΔG_{reg} are assumed to be 0.3 eV each. In order to theoretically predict efficiencies, one of the major assumptions that needs to be made relates to the required driving forces for charge injection and dye regeneration. Here, the authors note the simplicity of our model, however, it has been shown experimentally that in many systems, QE drops off rapidly when the energy offset is below a threshold value [148] as rates for forward and back transfer become less asymmetric. This is a broadly relevant question across all DSC research, and one which has been approached by a number of authors, as discussed below.

The advent of more stable ferrocene redox mediator systems for nDSC allowed Daeneke *et al.* [148] to investigate charge regeneration through the use of a series of ferrocene derivatives. Here it was seen that ΔG_{reg} values as small as 0.2-0.25 eV could provide near quantitative regeneration. Previously, Feldt *et al.* [217] had suggested a ΔG_{reg} value closer to 0.4 eV was necessary. This is explained in terms of the reorganisation energy of the redox mediator and suggests that it is possible this 'threshold' ΔG_{reg} of 0.2 eV may be further improved upon. Once again, the benefits of using single electron redox process can be seen as there is ~0.3-0.35 eV lost when using I^-/I_3^-. As discussed earlier (Figure 9), Gibson *et al.* [149] also investigated the role of ΔG_{reg} in pDSCs using I^-/I_3^- and a series of peryleneimide dyes. Below (Figure 18) device IPCE maxima are compared against ΔG_{reg}, where this value is determined as the energy difference between the dye reduction potential and the $I_2^{\bullet-}/I_3^-$ redox potential.

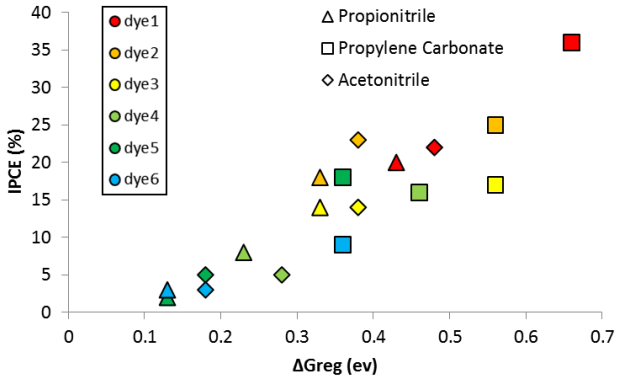

Figure 18 – regeneration driving force versus resultant IPCE for various perylene derivatives bound to NiO with I^-/I_3^- in different solvents (data from Gibson *et al.* [149]).

Similarly, the minimum required ΔG_{inj} for nDSCs has been investigated with a series of coumarin based sensitizers and TiO_2, by Hara *et al.* [218]. Based on IPCE values, they observed that as little as 150 meV may be required for near quantitative injection. On the other hand, a study by Mori *et al.* [75], using a similar approach, suggested a ΔG_{inj} of 0.6 eV was required for pDSCs. It is important to note that the dyes used in this study were not designed for pDSC application, suggesting that favourable electron distribution in the SOMO may substantially decrease the ΔG_{inj} requirements.

The dye O13, reported by Ji *et al.* in 2013 realised pDSC with $J_{SC} > 2.6$ mA/cm^2 with only ΔG_{inj} of 0.13 eV [92]. Even more impressive is the apparent ΔG_{inj} for the champion dye PMI-6T-TPA on NiO of less than 100

meV, based on electrochemical measurements [219]. This of course needs to be considered in the context of photoelectron spectroscopy in air [220] measurements, which suggest the work function of this dye to be -5.6 eV (versus vacuum) [183]. This ambiguity suggests that researchers in this field need to develop more appropriate measurements to determine *in situ* values. This is of course an issue that effects not just pDSC/pnDSC research, but rather the whole field of electrochemistry.

As was mentioned previously in Section 2.2, the required values of ΔG_{inj} and ΔG_{reg} may be different from each other. For the sake of this model these can be traded between the processes, (*e.g.* ΔG = 0.4 eV could account for either ΔG_{inj} = 0.2 eV and ΔG_{reg} = 0.2 eV or ΔG_{inj} = 0.1 eV and ΔG_{reg} = 0.3 eV). It is also assumed that reorganisation energies will be small and are also accounted for within these driving forces. Models with ΔG = 0.6 eV, 0.4 eV and 0.2 eV are presented for both single junction and tandem DSCs in Figure 19a. The other major assumption relates to the proximity of $_qE_f$ and the band edges. Here, it will be assumed that $_qE_F$ approximates the VB/CB edge for a photocathode/photoanode respectively. As noted previously, it is possible that with slow charge extraction and limited recombination, $_qE_F$ may reside below the VB edge / above the CB edge. For the purposes of this model, this would however be equivalent to selecting a dye with smaller driving force for charge injection.

Under operating conditions, $V_{OC} = (\lambda_2/h\upsilon) + (\lambda_3/h\upsilon) - (2 \cdot \Delta G)$. Here the FF was determined using the approximation provided by DeVos [214], at room temperature and assuming V_{OC} to be the offset between the CB edge of the n-type and VB of the p-type semiconductor.

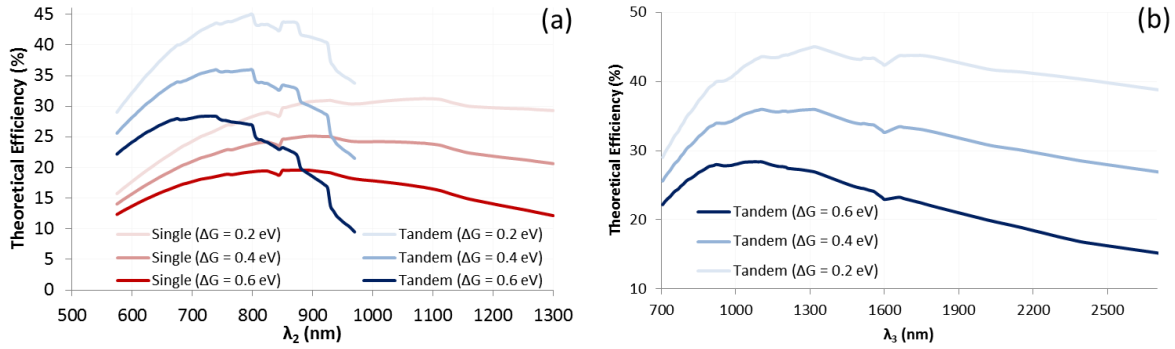

Figure 19 – Theoretical limiting efficiencies for single junction and tandem devices with different ΔG, as a function of (a) λ_2 (see Fig 15a) and (b) λ_3 in the case of tandem devices.

Obviously with optimal configuration, the tandem devices are capable of attaining higher efficiencies for a given ΔG, however, two points bear being explicitly stated. Firstly, the optimal λ_2 values for tandem devices are for relatively short wavelengths and secondly, as the ΔG values increase, this optimum is further blue shifted. Figure 19b illustrates the required λ_3 value to match the photon flux of the first electrode. If we are to take ΔG = 0.6 eV, an optimal configuration of pnDSC would have dye 1 absorbing to 730 nm and dye 2 to 1078 nm. This could provide a device with V_{OC} of 1.6 V and PCE of 28.4%, which is notably below the predicted theoretical limit (SQ) for a single junction device – highlighting the critical nature of decreasing such energy losses. With ΔG = 0.4 eV, λ_2 = 790 nm, λ_3 = 1290 nm a theoretically possible 34.9% PCE is realized. Corresponding ΔG values for single junction DSCs would suggest PCEs of 19.6% (880 nm onset) and 25.1 % (900 nm onset) respectively are possible.

If TiO_2 is retained as the n-type semiconductor, with (CB edge potential of ~ -4 eV), p-type materials with VB edge values (vacuum) of -6.13 eV, -5.73 eV or -5.65 eV would be required for ΔG = 0.2, 0.4 or 0.6 eV respectively. Redox mediators would of course need to be tuned in accordance with these energy levels.

Alternately TiO_2 may be replaced. To date only a handful of other n-type semiconductors have been used to create moderately successful nDSCs. These include ZnO [221], Nb_2O_5 [222] and Zn_2SnO_4 [223].

For the specific case of TiO_2 and NiO devices, the V_{OC} is set to 1100 mV, unless the aforementioned shift of ${}_qE_F$ into the VB/CB by a significant amount occurs. Experimental results of pnDSCs with a V_{OC} of 1079 mV suggest this may either occurring, or that the values (VB/CB edge potentials) measured *ex situ* are not the same *in situ* in a DSC.

If we assume this voltage (1.1 V) is approximately limiting, the maximum efficiency is therefore determined by the value of ΔG and the subsequent dye absorption ranges to which it corresponds. Figure 20, below, shows the theoretical device efficiency along with λ_3 as a function of ΔG. It can be seen for small driving forces the model finds its optimum deep into the IR (λ_3 = 4000 nm). The reason for this is that using these low energy photons (~0.3 eV) facilitates higher J_{SC}, as the normal situation of the trading off of current for voltage does not apply here. Even with this in mind, the 'best case' (with optimistic ΔG = 0.2 eV) provides slightly above what can be theoretically be obtained for a single junction device [45, 46] (and again below the SQ limit). This highlights that if NiO and TiO_2 remain locked in, the prospects for this system are indeed limited, a fact evidenced by the fact that redox mediators more positive than the VB edge of NiO can be used in nDSCs (such as Br^-/Br_3^-). These limitations were also recognized by Sobus and Ziolek in their analysis of theoretical device efficiencies for tandem DSCs [224].

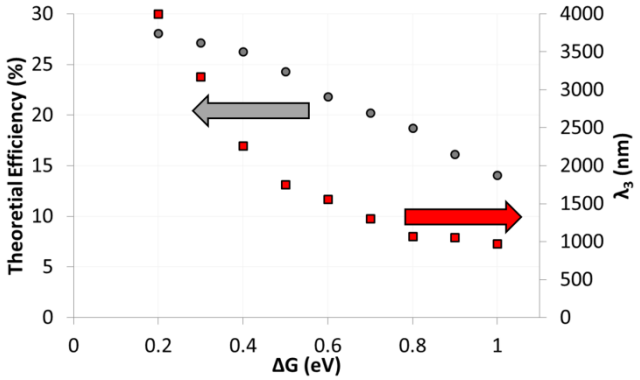

Figure 20 – Efficiency limit and required λ_3 to be employed to achieve said efficiency as a function of ΔG.

This modelling exercise demonstrates the substantial benefit which may be derived from pnDSC as opposed to single junction. In addition, module design may be aided from the low current, high voltage nature of tandems (lower series resistance losses).

3.3 RESEARCH PRIORITIES AND CONCLUSIONS

Throughout this article we have explored the remarkable progress that has occurred in the field of dye-sensitized photocathode research, with a 350-fold improvement in PCE between 1999 and 2015 [5, 84]. This has come about through development of nearly all components of the device. However, a number of limitations to pDSC performance still remain. These have also been examined, along with strategies to combat them. In addition to this, the possibility of very high pnDSC PCEs have been explored through a modelled system. In order to get close to these ideal performances, the previously mentioned limitations need to tackled. In our opinion one of the biggest issues are the energy losses associated the two electron redox processes of the I^-/I_3^- couple. Already

replacements for this have afforded substantial improvements. More broadly, the losses in potential experienced in DSCs are one of the chief limitations, and their minimization requires a great deal of attention.

Another critical aspect of pDSC development is the replacement of NiO with a material that can afford higher pnDSC V_{OC}s. Although this may also be achieved by replacing TiO_2, it is a very efficient and well understood system. Furthermore, NiO suffers from strong colouration (exacerbated by electrochromic properties) and trap states which facilitate recombination.

The third major issue to be addressed is the need for complimentary light harvesting. Recent development in redox mediators suggests that this challenge may be met either on the photocathode or the photoanode. Alongside this is the need to ensure electrochemical measurements are done such that they reflect the true environment of the materials in the device. It is also important to remember in the context of solar energy development that cross-fertilization can take place and may lead to even more radical redesigns and novel device architectures.

If we are to surpass the SQ limit, substantial improvements are required on both the pDSC and nDSC sides, although are a philosophical and economic question as to whether this must be the end goal for pnDSCs. Even if pnDSCs are not able to surpass the 31% PCE required to make them 3rd generation by the conventional metric (there is a question about what this threshold should be for DSCs, given the lack of a comprehensive theoretical model), the implementation of 3rd generation concepts should allow for substantial improvements in device performance as compared to single junction DSCs. The first examples of pDSCs led to a great deal of scepticism as to whether they would ever be good enough to combine with nDSCs to make these high efficiency devices, however recent developments show there is no fundamental reason why this can be achieved. It is also seen that researcher interest in this field has grown substantially - boding well for the technology.

4. Acknowdgements

The authors acknowledge the Australian Renewable Energy Agency (ARENA) and the Australian Centre for Advanced Photovoltaics. AN would like to acknolwdge fellowship support from ARENA (6-F020) and the Australian Research Council (DE160100504).

5. References

1. Kakiage, K., et al., *Highly-efficient dye-sensitized solar cells with collaborative sensitization by silyl-anchor and carboxy-anchor dyes.* Chemical Communications, 2015. **51**(88): p. 15894-15897.

2. Green, M.A., et al., *Solar cell efficiency tables (version 46).* Progress in Photovoltaics: Research and Applications, 2015. **23**(7): p. 805-812.

3. Green, M.A., *Third generation photovoltaics : advanced solar energy conversion*. 1st ed. 2003, New York: Springer. 160.

4. Shockley, W. and H.J. Queisser, *Detailed Balance Limit of Efficiency of p-n Junction Solar Cells.* Journal of Applied Physics, 1961. **32**(3): p. 10.

5. He, J.J., et al., *Dye-sensitized nanostructured p-type nickel oxide film as a photocathode for a solar cell.* Journal of Physical Chemistry B, 1999. **103**(42): p. 8940-8943.

6. He, J.J., et al., *Dye-sensitized nanostructured tandem cell-first demonstrated cell with a dye-sensitized photocathode.* Solar Energy Materials and Solar Cells, 2000. **62**(3): p. 265-273.

7. Bequerel, E., *Recherches sur les effets de la radiation chimique de la lumière solaire, au moyen des courants électriques.* Comptes Rendus de l'Académie des sciences, 1839. **9**: p. 145–149.

8. Einstein, A., *Über einen die Erzeugung und Verwandlung des Lichtes betreffenden heuristischen Gesichtspunkt.* Annalen der Physik, 1905. **322**(6): p. 132-148.

9. Moser, D.J., *Notiz über Verstärkung photoelektrischer Ströme durch optischel Sensibilisirung.* Akadem. Anzeiger, 1887. **16**.

10. Chapin, D.M., C.S. Fuller, and G.L. Pearson, *A New Silicon p-n Junction Photocell for Converting Solar Radiation into Electrical Power.* Journal of Applied Physics, 1954. **25**(5): p. 676-677.

11. Nelson, R.C., *Energy Transfers between Sensitizer and Substrate. III. Sensitization by Thick Dye Films*.* Journal of the Optical Society of America, 1961. **51**(11): p. 1182-1186.

12. Gerischer, H., et al., *Sensitization of Charge Injection Into Semiconductors with Large Band Gap.* Electrochimica Acta, 1968. **13**(6): p. 1509-&.

13. Fujishima, A. and K. Honda, *ELECTROCHEMICAL PHOTOLYSIS OF WATER AT A SEMICONDUCTOR ELECTRODE.* Nature, 1972. **238**(5358): p. 37-+.

14. Nozik, A.J., *Photoelectrochemistry - applications to solar-energy conversion.* Annual Review of Physical Chemistry, 1978. **29**: p. 189-222.

15. Bolts, J.M., et al., *Double photoelectrode-based cell for conversion of light to electricity - p-type CdTe and n-type CdSe photoelectrodes in a polysulfide electrolyte.* Journal of the American Chemical Society, 1977. **99**(14): p. 4826-4827.

16. Memming, R., *Photochemical and electrochemical processes of excited dyes at semiconductor and metal electrodes.* Photochemistry and Photobiology, 1972. **16**(4): p. 325.

17. Matsumura, M., et al., *Dye sensitization and surface-structures of semiconductor electrodes.* Industrial & Engineering Chemistry Product Research and Development, 1980. **19**(3): p. 415-421.

18. Fernando, C.A.N., et al., *Photoelectrochemical properties of rhodamine-C18 sensitized p-CuSCN photoelectrochemical Cell (PEC).* Solar Energy Materials and Solar Cells, 1994. **33**(3): p. 301-315.

19. Tennakone, K., et al., *The Characteristics of a para-CuCNS Photocathode Sensitzed with Acridine-Orange.* Solar Energy Materials, 1986. **14**(6): p. 499-506.

20. Tennakone, K., et al., *Dye Sensitization of Cuprous Thiocyanate Photocathodes in Aqueous KCNS.* Journal of the Electrochemical Society, 1984. **131**(7): p. 1574-1577.

21. O'Regan, B. and M. Graetzel, *A low-cost, high-efficiency solar-cell based on dye-sensitized colloidal TiO_2 films.* Nature, 1991. **353**: p. 737-740.

22. O'Regan, B. and D.T. Schwartz, *Efficient photo-hole injection from adsorbed cyanine dyes into electrodeposited copper(I) thiocyanate thin-films.* Chemistry of Materials, 1995. **7**(7): p. 1349-1354.

23. Anandan, S., X.G. Wen, and S.H. Yang, *Room temperature growth of CuO nanorod arrays on copper and their application as a cathode in dye-sensitized solar cells.* Materials Chemistry and Physics, 2005. **93**(1): p. 35-40.

24. Tennakone, K., et al., *Highly stable dye-sensitized solid-state solar cell with the semiconductor 4CuBr 3S(C_4H_9)$_2$ as the hole collector.* Applied Physics Letters, 2000. **77**(15): p. 2367-2369.

25. Tennakone, K., et al., *A Dye-Sensitized Nano-Porous Solid-State Photovoltaic Cell.* Semiconductor Science and Technology, 1995. **10**(12): p. 1689-1693.

26. Bandara, J. and J.P. Yasomanee, *p-type oxide semiconductors as hole collectors in dye-sensitized solid-state solar cells.* Semiconductor Science and Technology, 2007. **22**(2): p. 20-24.

27. Bandara, J., C.M. Divarathne, and S.D. Nanayakkara, *Fabrication of n-p junction electrodes made of n-type SnO2 and p-type NiO for control of charge recombination in dye sensitized solar cells.* Solar Energy Materials and Solar Cells, 2004. **81**(4): p. 429-437.

28. Nattestad, A., et al., *Highly efficient photocathodes for dye-sensitized tandem solar cells.* Nature Materials, 2010. **9**(1): p. 31-35.

29. Nakasa, A., et al., *Synthesis of porous nickel oxide nanofiber.* Chemistry Letters, 2005. **34**(3): p. 428-429.

30. Yu, M.Z., T.I. Draskovic, and Y.Y. Wu, *Cu(I)-based delafossite compounds as photocathodes in p-type dye-sensitized solar cells.* Physical Chemistry Chemical Physics, 2014. **16**(11): p. 5026-5033.

31. Odobel, F., et al., *New Photovoltaic Devices Based on the Sensitization of p-type Semiconductors: Challenges and Opportunities.* Accounts of Chemical Research, 2010. **43**(8): p. 1063-1071.

32. Odobel, F. and Y. Pellegrin, *Recent Advances in the Sensitization of Wide-Band-Gap Nanostructured p-Type Semiconductors. Photovoltaic and Photocatalytic Applications.* Journal of Physical Chemistry Letters, 2013. **4**(15): p. 2551-2564.

33. Odobel, F., et al., *Recent advances and future directions to optimize the performances of p-type dye-sensitized solar cells.* Coordination Chemistry Reviews, 2012. **256**(21–22): p. 2414-2423.

34. Buchalska, M., et al., *Photoinduced hole injection in semiconductor-coordination compound systems.* Coordination Chemistry Reviews, 2013. **257**(3-4): p. 767-775.

35. Shi, J.F., et al., *p-Type and pn-Type Dye-Sensitized Solar Cells.* Acta Physico-Chimica Sinica, 2011. **27**(6): p. 1287-1299.

36. Dini, D., et al., *The influence of the preparation method of NiO_x photocathodes on the efficiency of p-type dye-sensitized solar cells.* Coordination Chemistry Reviews, 2015. **304–305**: p. 179-201.

37. Borgstrom, M., et al., *Sensitized hole injection of phosphorus porphyrin into NiO: Toward new photovoltaic devices.* Journal of Physical Chemistry B, 2005. **109**(48): p. 22928-22934.

38. Morandeira, A., et al., *Photoinduced ultrafast dynamics of coumarin 343 sensitized p-type-nanostructured NiO films.* Journal of Physical Chemistry B, 2005. **109**(41): p. 19403-19410.

39. Qin, P., et al., *High Incident Photon-to-Current Conversion Efficiency of p-Type Dye-Sensitized Solar Cells Based on NiO and Organic Chromophores.* Advanced Materials, 2009. **21**(29): p. 2993-+.

40. Natu, G., et al., *The Effect of an Atomically Deposited Layer of Alumina on NiO in P-type Dye-Sensitized Solar Cells.* Langmuir, 2012. **28**(1): p. 950-956.

41. Uehara, S., et al., *Retardation of electron injection at NiO/dye/electrolyte interface by aluminium alkoxide treatment.* Energy & Environmental Science, 2010. **3**(5): p. 641-644.

42. Patel, P. *Dye-Sensitized Solar to Go: The low-cost cells make their debut on electronics-charging bags*. 2009 [cited 2015 November 23rd]; Available from: http://www.technologyreview.com/news/415912/dye-sensitized-solar-to-go/.

43. ASTM_International, *G173-03(2012) Standard Tables for Reference Solar Spectral Irradiances: Direct Normal and Hemispherical on 37° Tilted Surface*. 2012.

44. Henry, C.H., *Limiting efficiencies of ideal single and multiple energy-gap terrestrial solar-cells.* Journal of Applied Physics, 1980. **51**(8): p. 4494-4500.

45. Fingerhut, B.P., W. Zinth, and R. de Vivie-Riedle, *The detailed balance limit of photochemical energy conversion.* Physical Chemistry Chemical Physics, 2010. **12**(2): p. 422-432.

46. Tayebjee, M.J.Y., et al., *The efficiency limit of solar cells with molecular absorbers: A master equation approach.* Journal of Applied Physics, 2010. **108**(12).

47. Snaith, H.J., *Estimating the Maximum Attainable Efficiency in Dye-Sensitized Solar Cells.* Advanced Functional Materials, 2010. **20**(1): p. 13-19.

48. Goldschmidt, J.C. and S. Fischer, *Upconversion for Photovoltaics – a Review of Materials, Devices and Concepts for Performance Enhancement.* Advanced Optical Materials, 2015. **3**(4): p. 510-535.

49. Nattestad, A., et al., *Dye-Sensitized Solar Cell with Integrated Triplet-Triplet Annihilation Upconversion System.* Journal of Physical Chemistry Letters, 2013. **4**(12): p. 2073-2078.

50. Yuan, C., et al., *Use of colloidal upconversion nanocrystals for energy relay solar cell light harvesting in the near-infrared region.* Journal of Materials Chemistry, 2012. **22**(33): p. 16709-16713.

51. Hill, S.P., et al., *Photon Upconversion and Photocurrent Generation via Self-Assembly at Organic–Inorganic Interfaces.* The Journal of Physical Chemistry Letters, 2015. **6**(22): p. 4510-4517.

52. Simpson, C., et al., *An intermediate band dye-sensitised solar cell using triplet-triplet annihilation.* Physical Chemistry Chemical Physics, 2015. **17**(38): p. 24826-24830.

53. Sambur, J.B., T. Novet, and B.A. Parkinson, *Multiple Exciton Collection in a Sensitized Photovoltaic System.* Science, 2010. **330**(6000): p. 63-66.

54. Durr, M., et al., *Tandem dye-sensitized solar cell for improved power conversion efficiencies.* Applied Physics Letters, 2004. **84**(17): p. 3397-3399.

55. Kubo, W., et al., *Dye-sensitized solar cells: improvement of spectral response by tandem structure.* Journal of Photochemistry and Photobiology A - Chemistry, 2004. **164**(1-3): p. 33-39.

56. Li, L., et al., *A Double-Band Tandem Organic Dye-sensitized Solar Cell with an Efficiency of 11.5 %.* ChemSusChem, 2011. **4**(5): p. 609-612.

57. Murayama, M. and T. Mori, *Dye-sensitized solar cell using novel tandem cell structure.* Journal of Physics D - Applied Physics, 2007. **40**(6): p. 1664-1668.

58. Liska, P., et al., *Nanocrystalline dye-sensitized solar cell/copper indium gallium selenide thin-film tandem showing greater than 15% conversion efficiency.* Applied Physics Letters, 2006. **88**(20): p. 203103.

59. Bruder, I., et al., *Efficient organic tandem cell combining a solid state dye-sensitized and a vacuum deposited bulk heterojunction solar cell.* Solar Energy Materials and Solar Cells, 2009. **93**(10): p. 1896-1899.

60. Chiba, Y., et al., *Dye-sensitized solar cells with conversion efficiency of 11.1%.* Japanese Journal of Applied Physics Part 2 - Letters & Express Letters, 2006. **45**(24-28): p. L638-L640.

61. Yu, Q., et al., *High-Efficiency Dye-Sensitized Solar Cells: The Influence of Lithium Ions on Exciton Dissociation, Charge Recombination, and Surface States.* Acs Nano, 2010. **4**(10): p. 6032-6038.

62. Yella, A., et al., *Porphyrin-Sensitized Solar Cells with Cobalt (II/III)–Based Redox Electrolyte Exceed 12 Percent Efficiency.* Science, 2011. **334**(6056): p. 629-634.

63. Mathew, S., et al., *Dye-sensitized solar cells with 13% efficiency achieved through the molecular engineering of porphyrin sensitizers.* Nature Chemistry, 2014. **6**(3): p. 242-247.

64. Gibson, E.A., et al., *Cobalt Polypyridyl-Based Electrolytes for p-Type Dye-Sensitized Solar Cells.* Journal of Physical Chemistry C, 2011. **115**(19): p. 9772-9779.

65. Powar, S., et al., *Improved Photovoltages for p-Type Dye-Sensitized Solar Cells Using $CuCrO_2$ Nanoparticles.* Journal of Physical Chemistry C, 2014. **118**(30): p. 16375-16379.

66. Xu, X.B., et al., *Near Field Enhanced Photocurrent Generation in P-type Dye-Sensitized Solar Cells.* Scientific Reports, 2014. **4**.

67. Kroon, J.M., et al., *Nanocrystalline dye-sensitized solar cells having maximum performance.* Progress in Photovoltaics, 2007. **15**(1): p. 1-18.

68. Dyeamo_AB. *Organic DSSC dyes*. 2015 [cited 2015 December 2nd]; Available from: http://dyenamo.se/dyenamo_dyes.php#dnfpseries.

69. Favereau, L., et al., *Diketopyrrolopyrrole derivatives for efficient NiO-based dye-sensitized solar cells.* Chemical Communications, 2013. **49**(73): p. 8018-8020.

70. Flynn, C.J., et al., *Hierarchically-Structured NiO Nanoplatelets as Mesoscale p-Type Photocathodes for Dye-Sensitized Solar Cells.* Journal of Physical Chemistry C, 2014. **118**(26): p. 14177-14184.

71. He, X.X., et al., *Synthesis of Nest-Like NiO and Its Application on P-Type Dye-Sensitized Solar Cell*, in *Materials for Energy Conversion and Storage*, H. Zhang, Editor. 2012, Trans Tech Publications Ltd: Stafa-Zurich. p. 61-64.

72. Hod, I., et al., *Characterization and control of the electronic properties of a NiO based dye sensitized photocathode.* Physical Chemistry Chemical Physics, 2013. **15**(17): p. 6339-6343.

73. Macdonald, T.J., et al., *$CuInS_2$/ZnS nanocrystals as sensitisers for NiO photocathodes.* Journal of Materials Chemistry A, 2015. **3**(25): p. 13324-13331.

74. Mizoguchi, Y. and S. Fujihara, *Fabrication and dye-sensitized solar cell performance of nanostructured NiO/coumarin 343 photocathodes.* Electrochemical and Solid State Letters, 2008. **11**(8): p. K78-K80.

75. Mori, S., et al., *Charge-Transfer Processes in Dye-Sensitized NiO Solar Cells.* Journal of Physical Chemistry C, 2008. **112**(41): p. 16134-16139.

76. Nattestad, A., et al., *Dye-sensitized nickel(II) oxide photocathodes for tandem solar cell applications.* Nanotechnology, 2008. **19**(29).

77. Wu, Q., et al., *Morphology and properties of NiO electrodes for p-DSSCs based on hydrothermal method.* Applied Surface Science, 2013. **276**: p. 411-416.

78. Zhu, H., A. Hagfeldt, and G. Boschloo, *Photoelectrochemistry of mesoporous NiO electrodes in Iodide/Triiodide electrolytes.* Journal of Physical Chemistry C, 2007. **111**(47): p. 17455-17458.

79. Park, J.Y., et al., *Influence of the anchoring number in a carbazole-based photosensitizer on the photovoltaic performance of p-type NiO dye sensitized solar cells.* Rsc Advances, 2014. **4**(106): p. 61248-61255.

80. Morandeira, A., et al., *Improved Photon-to-Current Conversion Efficiency with a Nanoporous p-Type NiO Electrode by the Use of a Sensitizer-Acceptor Dyad.* The Journal of Physical Chemistry C, 2008. **112**(5): p. 1721-1728.

81. Qin, P., et al., *Design of an organic chromophore for p-type dye-sensitized solar cells.* Journal of the American Chemical Society, 2008. **130**(27): p. 8570-+.

82. Qin, P., et al., *Synthesis and Mechanistic Studies of Organic Chromophores with Different Energy Levels for p-Type Dye-Sensitized Solar Cells.* Journal of Physical Chemistry C, 2010. **114**(10): p. 4738-4748.

83. Zhang, X.L., et al., *Enhanced open-circuit voltage of p-type DSC with highly crystalline NiO nanoparticles.* Chemical Communications, 2011. **47**(16): p. 4808-4810.

84. Perera, I.R., et al., *Application of the Tris(acetylacetonato)iron(III)/(II) Redox Couple in p-Type Dye-Sensitized Solar Cells.* Angewandte Chemie-International Edition, 2015. **54**(12): p. 3758-3762.

85. Powar, S., et al., *Highly Efficient p-Type Dye-Sensitized Solar Cells based on Tris(1,2-diaminoethane)Cobalt(II)/(III) Electrolytes.* Angewandte Chemie-International Edition, 2013. **52**(2): p. 602-605.

86. Enea, O., J. Moser, and M. Grätzel, *Achievement of incident photon to electric current conversion yields exceeding 80% in the spectral sensitization of titanium dioxide by coumarin.* Journal of Electroanalytical Chemistry and Interfacial Electrochemistry, 1989. **259**(1): p. 59-65.

87. Warnan, J., et al., *Multichromophoric Sensitizers Based on Squaraine for NiO Based Dye-Sensitized Solar Cells.* Journal of Physical Chemistry C, 2014. **118**(1): p. 103-113.

88. Wood, C.J., et al., *Red-Absorbing Cationic Acceptor Dyes for Photocathodes in Tandem Solar Cells.* Journal of Physical Chemistry C, 2014. **118**(30): p. 16536-16546.

89. Zhang, Q.Q., et al., *A push-pull thienoquinoidal chromophore for highly efficient p-type dye-sensitized solar cells.* Journal of Materials Chemistry A, 2015. **3**(15): p. 7695-7698.

90. Ji, Z.Q., et al., *Linker effect in organic donor-acceptor dyes for p-type NiO dye sensitized solar cells.* Energy & Environmental Science, 2011. **4**(8): p. 2818-2821.

91. Shi, Z., et al., *$NiCo_2O_4$ Nanostructures as a Promising Alternative for NiO Photocathodes in p-Type Dye-Sensitized Solar Cells with High Efficiency.* Energy Technology, 2014. **2**(6): p. 517-521.

92. Ji, Z.Q., G. Natu, and Y.Y. Wu, *Cyclometalated Ruthenium Sensitizers Bearing a Triphenylamino Group for p-Type NiO Dye-Sensitized Solar Cells.* Acs Applied Materials & Interfaces, 2013. **5**(17): p. 8641-8648.

93. Mishra, A., M.K.R. Fischer, and P. Bäuerle, *Metal-Free Organic Dyes for Dye-Sensitized Solar Cells: From Structure: Property Relationships to Design Rules.* Angewandte Chemie International Edition, 2009. **48**(14): p. 2474-2499.

94. Weidelener, M., et al., *Synthesis and Characterization of Organic Dyes with Various Electron-Accepting Substituents for p-Type Dye-Sensitized Solar Cells.* Chemistry-an Asian Journal, 2014. **9**(11): p. 3251-3263.

95. Wu, F., et al., *D-A-A-Type Organic Dyes for NiO-Based Dye-Sensitized Solar Cells.* European Journal of Organic Chemistry, 2015(31): p. 6850-6857.

96. Yen, Y.-S., et al., *Arylamine-Based Dyes for p-Type Dye-Sensitized Solar Cells.* Organic Letters, 2011. **13**(18): p. 4930-4933.

97. Zhu, L.N., et al., *Rational design of triphenylamine dyes for highly efficient p-type dye sensitized solar cells.* Dyes and Pigments, 2014. **105**: p. 97-104.

98. Wood, C.J., G.H. Summers, and E.A. Gibson, *Increased photocurrent in a tandem dye-sensitized solar cell by modifications in push-pull dye-design.* Chemical Communications, 2015. **51**(18): p. 3915-3918.

99. Li, H.B., et al., *Theoretical study and design of triphenylamine-malononitrile-based p-type organic dyes with different pi-linkers for dyes-sensitized solar cells.* Dyes and Pigments, 2014. **108**: p. 106-114.

100. Wang, X. and D.M. Stanbury, *Oxidation of Iodide by a Series of Fe(III) Complexes in Acetonitrile.* Inorganic Chemistry, 2006. **45**(8): p. 3415-3423.

101. Weidelener, M., et al., *Synthesis and characterization of perylene-bithiophene-triphenylamine triads: studies on the effect of alkyl-substitution in p-type NiO based photocathodes.* Journal of Materials Chemistry, 2012. **22**(15): p. 7366-7379.

102. Cui, J., et al., *Organic Sensitizers with Pyridine Ring Anchoring Group for p-Type Dye-Sensitized Solar Cells.* Journal of Physical Chemistry C, 2014. **118**(30): p. 16433-16440.

103. Liu, Z.H., et al., *Modulated Charge Injection in p-Type Dye-Sensitized Solar Cells Using Fluorene-Based Light Absorbers.* Acs Applied Materials & Interfaces, 2014. **6**(5): p. 3448-3454.

104. Le Pleux, L., et al., *Synthesis, photophysical and photovoltaic investigations of acceptor-functionalized perylene monoimide dyes for nickel oxide p-type dye-sensitized solar cells.* Energy & Environmental Science, 2011. **4**(6): p. 2075-2084.

105. Click, K.A., et al., *A double-acceptor as a superior organic dye design for p-type DSSCs: high photocurrents and the observed light soaking effect.* Physical Chemistry Chemical Physics, 2014. **16**(47): p. 26103-26111.

106. Chang, C.H., et al., *Squaraine-Arylamine Sensitizers for Highly Efficient p-Type Dye-Sensitized Solar Cells.* Organic Letters, 2012. **14**(18): p. 4726-4729.

107. Pellegrin, Y., et al., *Ruthenium polypyridine complexes as sensitizers in NiO based p-type dye-sensitized solar cells: Effects of the anchoring groups.* Journal of Photochemistry and Photobiology a-Chemistry, 2011. **219**(2-3): p. 235-242.

108. Anne, F.B., N. Galland, and D. Jacquemin, *Computing redox potentials for dyes used in p-type dye-sensitized solar cells.* International Journal of Quantum Chemistry, 2012. **112**(24): p. 3763-3768.

109. Munoz-Garcia, A.B. and M. Pavone, *Structure and energy level alignment at the dye-electrode interface in p-type DSSCs: new hints on the role of anchoring modes from ab initio calculations.* Physical Chemistry Chemical Physics, 2015. **17**(18): p. 12238-12246.

110. Sheehan, S., et al., *Comparison of the photoelectrochemical properties of RDS NiO thin films for p-type DSCs with different organic and organometallic dye-sensitizers and evidence of a direct correlation between cell efficiency and charge recombination.* Journal of Solid State Electrochemistry, 2015. **19**(4): p. 975-986.

111. Ursu, D., et al., *Impact of Fe doping on performances of $CuGaO_2$ p-type dye-sensitized solar cells.* Materials Letters, 2015. **143**: p. 91-93.

112. Clifford, J.N., et al., *Dye Dependent Regeneration Dynamics in Dye Sensitized Nanocrystalline Solar Cells: Evidence for the Formation of a Ruthenium Bipyridyl Cation/Iodide Intermediate.* The Journal of Physical Chemistry C, 2007. **111**(17): p. 6561-6567.

113. Kusama, H., H. Sugihara, and K. Sayama, *Effect of Cations on the Interactions of Ru Dye and Iodides in Dye-Sensitized Solar Cells: A Density Functional Theory Study.* The Journal of Physical Chemistry C, 2011. **115**(5): p. 2544-2552.

114. Freys, J.C., et al., *Ru-based donor-acceptor photosensitizer that retards charge recombination in a p-type dye-sensitized solar cell.* Dalton Transactions, 2012. **41**(42): p. 13105-13111.

115. Wood, C.J., et al., *Novel triphenylamine-modified ruthenium(II) terpyridine complexes for nickel oxide-based cathodic dye-sensitized solar cells.* Rsc Advances, 2014. **4**(11): p. 5782-5791.

116. Huang, Z., et al., *Dye-Controlled Interfacial Electron Transfer for High-Current Indium Tin Oxide Photocathodes.* Angewandte Chemie-International Edition, 2015. **54**(23): p. 6857-6861.

117. Sun, L.L., et al., *Exploring the influence of electron donating/withdrawing groups on hexamolybdate-based derivatives for efficient p-type dye-sensitized solar cells (DSSCs).* Rsc Advances, 2015. **5**(50): p. 39821-39827.

118. Rhee, J.H., et al., *Cu_2S-deposited mesoporous NiO photocathode for a solar cell.* Chemical Physics Letters, 2009. **477**(4-6): p. 345-348.

119. Chan, X.-H., et al., *Characteristics of p-NiO Thin Films Prepared by Spray Pyrolysis and Their Application in CdS-sensitized Photocathodes.* Journal of the Electrochemical Society, 2011. **158**(7): p. H733-H740.

120. Barceló, I., et al., *Preparation and Characterization of Nickel Oxide Photocathodes Sensitized with Colloidal Cadmium Selenide Quantum Dots.* Journal of Physical Chemistry C, 2013. **117**(44): p. 22509-22517.

121. Safari-Alamuti, F., et al., *Conformal growth of nanocrystalline CdX (X = S, Se) on mesoscopic NiO and their photoelectrochemical properties.* Physical Chemistry Chemical Physics, 2013. **15**(13): p. 4767-4774.

122. Kang, S.H., et al., *Hole transport in sensitized CdS-NiO nanoparticle photocathodes.* Chemical Communications, 2011. **47**(37): p. 10419-10421.

123. Mao, Y.Q., et al., *P-type CoO nanowire arrays and their application in quantum dot-sensitized solar cells.* Rsc Advances, 2013. **3**(4): p. 1217-1221.

124. Park, M.A., et al., *CdSe Quantum Dot-sensitized, Nanoporous p-type NiO Photocathodes for Quantum Dot-sensitized Solar Cells.* Molecular Crystals and Liquid Crystals, 2014. **598**(1): p. 154-162.

125. Park, M.A., et al., *Enhanced photoelectrochemical response of CdSe quantum dot-sensitized p-type NiO photocathodes.* Physica Status Solidi a-Applications and Materials Science, 2014. **211**(8): p. 1868-1872.

126. Tian, H., et al., *Solid-State Perovskite-Sensitized p-Type Mesoporous Nickel Oxide Solar Cells.* Chemsuschem, 2014. **7**(8): p. 2150-2153.

127. Wang, H., et al., *Boosting the Photocurrent Density of p-Type Solar Cells Based on Organometal Halide Perovskite-Sensitized Mesoporous NiO Photocathodes.* Acs Applied Materials & Interfaces, 2014. **6**(15): p. 12609-12617.

128. Im, J.-H., et al., *6.5% efficient perovskite quantum-dot-sensitized solar cell.* Nanoscale, 2011. **3**(10): p. 4088-4093.

129. Lee, M.M., et al., *Efficient Hybrid Solar Cells Based on Meso-Superstructured Organometal Halide Perovskites.* Science, 2012. **338**(6107): p. 643-647.

130. Liu, M., M.B. Johnston, and H.J. Snaith, *Efficient planar heterojunction perovskite solar cells by vapour deposition.* Nature, 2013. **advance online publication**.

131. Wang, K.-C., et al., *p-type Mesoscopic Nickel Oxide/Organometallic Perovskite Heterojunction Solar Cells.* Scientific Reports, 2014. **4**.

132. Jeng, J.-Y., et al., *Nickel Oxide Electrode Interlayer in $CH_3NH_3PbI_3$ Perovskite/PCBM Planar-Heterojunction Hybrid Solar Cells.* Advanced Materials, 2014. **26**(24): p. 4107-4113.

133. Liu, Z., et al., *p-Type mesoscopic NiO as an active interfacial layer for carbon counter electrode based perovskite solar cells.* Dalton Transactions, 2015. **44**(9): p. 3967-3973.

134. Zhang, J., et al., *Influence of highly efficient PbS counter electrode on photovoltaic performance of CdSe quantum dots-sensitized solar cells.* Journal of Solid State Electrochemistry, 2013. **17**(11): p. 2909-2915.

135. Qian, J., et al., *A Selenium-Based Cathode for a High-Voltage Tandem Photoelectrochemical Solar Cell.* Angewandte Chemie-International Edition, 2012. **51**(41): p. 10351-10354.

136. Lin, C.-Y., et al., *Photoactive p-type PbS as a counter electrode for quantum dot-sensitized solar cells.* Journal of Materials Chemistry A, 2013. **1**(4): p. 1155-1162.

137. Sumikura, S., et al., *Photoelectrochemical characteristics of cells with dyed and undyed nanoporous p-type semiconductor CuO electrodes.* Journal of Photochemistry and Photobiology a-Chemistry, 2008. **194**(2-3): p. 143-147.

138. Burke, A., et al., *A novel blue dye for near-IR 'dye-sensitised' solar cell applications.* Chemical Communications, 2007(3): p. 234-236.

139. Amao, Y. and Y. Yamada, *Near-IR light-sensitized voltaic conversion system using nanocrystalline TiO_2 film by Zn chlorophyll derivative aggregated.* Langmuir, 2005. **21**(7): p. 3008-3012.

140. Tian, H.N., et al., *A metal-free "black dye'' for panchromatic dye-sensitized solar cells.* Energy & Environmental Science, 2009. **2**(6): p. 674-677.

141. Li, C., et al., *para-dialkylaminophenyl dyes for efficient nanocrystalline TiO2 sensitization in far-red region.* Chinese Journal of Chemistry, 2006. **24**(4): p. 537-545.

142. Ono, T., T. Yamaguchi, and H. Arakawa, *Influence of Dye Adsorption Solvent on the Performance of a Mesoporous TiO2 Dye-Sensitized Solar Cell Using Infrared Organic Dye.* Journal of Solar Energy Engineering, 2010. **132**(2): p. 021101-021101.

143. Hamann, T.W. and J.W. Ondersma, *Dye-sensitized solar cell redox shuttles.* Energy & Environmental Science, 2011. **4**(2): p. 370-381.

144. Wang, M., et al., *Recent developments in redox electrolytes for dye-sensitized solar cells.* Energy Environ. Sci., 2012. **5**(11): p. 9394-9405.

145. Zhang, X.L., et al., *Sensitization of nickel oxide: improved carrier lifetime and charge collection by tuning nanoscale crystallinity.* Chemical Communications, 2012. **48**(79): p. 9885-9887.

146. Wang, Z.S., K. Sayama, and H. Sugihara, *Efficient eosin Y dye-sensitized solar cell containing Br^-/Br_3^- electrolyte.* Journal of Physical Chemistry B, 2005. **109**(47): p. 22449-22455.

147. Hara, K., et al., *Highly efficient photon-to-electron conversion with mercurochrome-sensitized nanoporous oxide semiconductor solar cells.* Solar Energy Materials and Solar Cells, 2000. **64**(2): p. 115-134.

148. Daeneke, T., et al., *Dye regeneration and charge recombination in dye-sensitized solar cells with ferrocene derivatives as redox mediators.* Energy & Environmental Science, 2012. **5**(5): p. 7090-7099.

149. Gibson, E.A., et al., *Role of the Triiodide/Iodide Redox Couple in Dye Regeneration in p-Type Dye-Sensitized Solar Cells.* Langmuir, 2012. **28**(15): p. 6485-6493.

150. Boschloo, G. and A. Hagfeldt, *Characteristics of the Iodide/Triiodide Redox Mediator in Dye-Sensitized Solar Cells.* Accounts of Chemical Research, 2009. **42**(11): p. 1819-1826.

151. Matsuda, T. and H. Matsumoto, *Influence of the iodine content on the photocurrent in dye-sensitized solar cells using liquid polyiodide.* Electrochemistry, 2002. **70**(6): p. 446-448.

152. Loos, K.R. and A.C. Jones, *Structure of triiodide ion in solution. Raman evidence for the existence of higher polyiodide species.* The Journal of Physical Chemistry, 1974. **78**(22): p. 2306-2307.

153. Svensson, P.H. and L. Kloo, *Synthesis, Structure, and Bonding in Polyiodide and Metal Iodide−Iodine Systems.* Chemical Reviews, 2003. **103**(5): p. 1649-1684.

154. Nattestad, A., *Development of photocathodes for incorporation into tandem dye sensitised solar cells*.

155. Gibson, E.A., et al., *A p-Type NiO-Based Dye-Sensitized Solar Cell with an Open-Circuit Voltage of 0.35 V.* Angewandte Chemie-International Edition, 2009. **48**(24): p. 4402-4405.

156. Xu, X., et al., *Efficient p-type dye-sensitized solar cells based on disulfide/thiolate electrolytes.* Nanoscale, 2013. **5**(17): p. 7963-7969.

157. Wang, M., et al., *An organic redox electrolyte to rival triiodide/iodide in dye-sensitized solar cells.* Nat Chem, 2010. **2**(5): p. 385-389.

158. Pavlishchuk, V.V. and A.W. Addison, *Conversion constants for redox potentials measured versus different reference electrodes in acetonitrile solutions at 25 degrees C.* Inorganica Chimica Acta, 2000. **298**(1): p. 97-102.

159. Fischer, A., et al., *Crystal formation involving 1-methylbenzimidazole in iodide/triiodide electrolytes for dye-sensitized solar cells.* Solar Energy Materials and Solar Cells, 2007. **91**(12): p. 1062-1065.

160. Xu, K., *Nonaqueous Liquid Electrolytes for Lithium-Based Rechargeable Batteries.* Chemical Reviews, 2004. **104**(10): p. 4303-4418.

161. Yu, Z., et al., *Liquid electrolytes for dye-sensitized solar cells.* Dalton Transactions, 2011. **40**(40): p. 10289-10303.

162. Wu, J., et al., *Electrolytes in Dye-Sensitized Solar Cells.* Chemical Reviews, 2015. **115**(5): p. 2136-2173.

163. Hagfeldt, A., et al., *Dye-Sensitized Solar Cells.* Chemical Reviews, 2010. **110**(11): p. 6595-6663.

164. Nazeeruddin, M.K., et al., *Conversion of light to electricity by cis-X_2bis(2,2'-bipyridyl-4,4'-dicarboxylate)ruthenium(II) charge-transfer sensitizers (X = Cl^-, Br^-, I^-, CN^-, and SCN^-) on nanocrystalline TiO_2 electrodes.* Journal of the American Chemical Society, 1993. **115**(14): p. 6382-6390.

165. Grätzel, M., *Dye-sensitized solar cells.* Journal of Photochemistry and Photobiology C: Photochemistry Reviews, 2003. **4**(2): p. 145-153.

166. Zhang, L., et al., *Solid state p-type dye-sensitized solar cells: concept, experiment and mechanism.* Physical Chemistry Chemical Physics, 2015.

167. Huang, S.Y., et al., *Charge Recombination in Dye-Sensitized Nanocrystalline TiO_2 Solar Cells.* The Journal of Physical Chemistry B, 1997. **101**(14): p. 2576-2582.

168. Stergiopoulos, T., et al., *Influence of electrolyte co-additives on the performance of dye-sensitized solar cells.* Nanoscale Research Letters, 2011. **6**.

169. Yin, X., et al., *The effects of pyridine derivative additives on interface processes at nanocrystalline TiO_2 thin film in dye-sensitized solar cells.* Surface and Interface Analysis, 2007. **39**(10): p. 809-816.

170. Schlichthörl, G., et al., *Band Edge Movement and Recombination Kinetics in Dye-Sensitized Nanocrystalline TiO_2 Solar Cells: A Study by Intensity Modulated Photovoltage Spectroscopy.* The Journal of Physical Chemistry B, 1997. **101**(41): p. 8141-8155.

171. Boschloo, G., L. Häggman, and A. Hagfeldt, *Quantification of the Effect of 4-tert-Butylpyridine Addition to I^-/I_3^- Redox Electrolytes in Dye-Sensitized Nanostructured TiO_2 Solar Cells.* The Journal of Physical Chemistry B, 2006. **110**(26): p. 13144-13150.

172. Vera, F., et al., *Preparation and characterization of eosin B- and Erythrosin J-sensitized nanostructured NiO thin film photocathodes.* Thin Solid Films, 2005. **490**(2): p. 182-188.

173. Lepleux, L., et al., *Simple and Reproducible Procedure to Prepare Self-Nanostructured NiO Films for the Fabrication of P-Type Dye-Sensitized Solar Cells.* Inorganic Chemistry, 2009. **48**(17): p. 8245-8250.

174. Awais, M., et al., *Spray-deposited NiO (x) films on ITO substrates as photoactive electrodes for p-type dye-sensitized solar cells.* Journal of Applied Electrochemistry, 2013. **43**(2): p. 191-197.

175. Li, C.Y. and S.X. Liu, *Preparation and Characterization of $Ni(OH)_2$ and NiO Mesoporous Nanosheets.* Journal of Nanomaterials, 2012.

176. Powar, S., et al., *Improved photocurrents for p-type dye-sensitized solar cells using nano-structured nickel(II) oxide microballs.* Energy & Environmental Science, 2012. **5**(10): p. 8896-8900.

177. Choi, H., et al., *The construction of tandem dye-sensitized solar cells from chemically-derived nanoporous photoelectrodes.* Journal of Power Sources, 2015. **274**: p. 937-942.

178. Smeigh, A.L., et al., *Ultrafast recombination for NiO sensitized with a series of perylene imide sensitizers exhibiting Marcus normal behaviour.* Chemical Communications, 2012. **48**(5): p. 678-680.

179. D'Amario, L., et al., *Tuning of Conductivity and Density of States of NiO Mesoporous Films Used in p-Type DSSCs.* Journal of Physical Chemistry C, 2014. **118**(34): p. 19556-19564.

180. Wang, H.T., et al., *p-Type dye-sensitized solar cell based on nickel oxide photocathode with or without Li doping.* Journal of Alloys and Compounds, 2014. **584**: p. 142-147.

181. Natu, G., et al., *Valence Band-Edge Engineering of Nickel Oxide Nanoparticles via Cobalt Doping for Application in p-Type Dye-Sensitized Solar Cells.* Acs Applied Materials & Interfaces, 2012. **4**(11): p. 5922-5929.

182. Huang, Z., et al., *Enhanced performance of p-type dye sensitized solar cells based on mesoporous $Ni_{1-x}Mg_xO$ ternary oxide films.* Rsc Advances, 2014. **4**(105): p. 60670-60674.

183. Nattestad, A., et al., *Dye-sensitized $CuAlO_2$ photocathodes for tandem solar cell applications.* Journal of Photonics for Energy, 2011. **1**.

184. Xiong, D., et al., *Hydrothermal synthesis of ultrasmall $CuCrO_2$ nanocrystal alternatives to NiO nanoparticles in efficient p-type dye-sensitized solar cells.* Journal of Materials Chemistry, 2012. **22**(47): p. 24760-24768.

185. Xu, Z., et al., *Remarkable photocurrent of p-type dye-sensitized solar cell achieved by size controlled $CuGaO_2$ nanoplates.* Journal of Materials Chemistry A, 2014. **2**(9): p. 2968-2976.

186. Chen, P., et al., *High Open-Circuit Voltage Solid-State Dye-Sensitized Solar Cells with Organic Dye.* Nano Letters, 2009. **9**(6): p. 2487-2492.

187. Bandara, J. and H. Weerasinghe, *Solid-state dye-sensitized solar cell with p-type NiO as a hole collector.* Solar Energy Materials and Solar Cells, 2005. **85**(3): p. 385-390.

188. Guo, Y., et al., *Enhanced performance of NiMgO-based ultraviolet photodetector by rapid thermal annealing.* Thin Solid Films, 2014. **558**: p. 311-314.

189. Krawicz, A., D. Cedeno, and G.F. Moore, *Energetics and efficiency analysis of a cobaloxime-modified semiconductor under simulated air mass 1.5 illumination.* Physical Chemistry Chemical Physics, 2014. **16**(30): p. 15818-15824.

190. Xu, Y. and M.A.A. Schoonen, *The absolute energy positions of conduction and valence bands of selected semiconducting minerals.* American Mineralogist, 2000. **85**(3-4): p. 543-556.

191. Allegrucci, A., et al., *Improved performance of porphyrin-based dye sensitised solar cells by phosphinic acid surface treatment.* Energy & Environmental Science, 2009. **2**(10): p. 1069-1073.

192. Zakeeruddin, S.M., et al., *Design, Synthesis, and Application of Amphiphilic Ruthenium Polypyridyl Photosensitizers in Solar Cells Based on Nanocrystalline TiO2 Films.* Langmuir, 2002. **18**(3): p. 952-954.

193. Kay, A. and M. Gratzel, *Dye-sensitized core-shell nanocrystals: Improved efficiency of mesoporous tin oxide electrodes coated with a thin layer of an insulating oxide.* Chemistry of Materials, 2002. **14**(7): p. 2930-2935.

194. Kay, A. and M. Grätzel, *Dye-Sensitized Core−Shell Nanocrystals: Improved Efficiency of Mesoporous Tin Oxide Electrodes Coated with a Thin Layer of an Insulating Oxide.* Chemistry of Materials, 2002. **14**(7): p. 2930-2935.

195. Chitambar, M., et al., *Dye-Sensitized Photocathodes: Efficient Light-Stimulated Hole Injection into p-GaP Under Depletion Conditions.* Journal of the American Chemical Society, 2012. **134**(25): p. 10670-10681.

196. Nakabayashi, S., N. Ohta, and A. Fujishima, *Dye sensitization of synthetic p-type diamond electrode.* Physical Chemistry Chemical Physics, 1999. **1**(17): p. 3993-3997.

197. Takechi, K., et al., *A Z-scheme type photoelectrochemical cell consisting of porphyrin-containing polymer and dye-sensitized TiO_2 electrodes.* Photochemical & Photobiological Sciences, 2010. **9**(8): p. 1085-1087.

198. Splan, K.E., A.M. Massari, and J.T. Hupp, *A Porous Multilayer Dye-Based Photoelectrochemical Cell That Unexpectedly Runs in Reverse.* The Journal of Physical Chemistry B, 2004. **108**(13): p. 4111-4115.

199. Chavhan, S.I., et al., *Sensitization of p-type NiO Using n-type Conducting Polymers.* Journal of Physical Chemistry C, 2010. **114**(45): p. 19496-19502.

200. Manders, J.R., et al., *Solution-Processed Nickel Oxide Hole Transport Layers in High Efficiency Polymer Photovoltaic Cells.* Advanced Functional Materials, 2013. **23**(23): p. 2993-3001.

201. Li, M.-H., et al., *Inorganic p-type contact materials for perovskite-based solar cells.* Journal of Materials Chemistry A, 2015. **3**(17): p. 9011-9019.

202. Li, L., et al., *Visible light driven hydrogen production from a photo-active cathode based on a molecular catalyst and organic dye-sensitized p-type nanostructured NiO.* Chemical Communications, 2012. **48**(7): p. 988-990.

203. Tong, L., et al., *Sustained solar hydrogen generation using a dye-sensitised NiO photocathode/$BiVO_4$ tandem photo-electrochemical device.* Energy & Environmental Science, 2012. **5**(11): p. 9472-9475.

204. Li, F., et al., *Organic Dye-Sensitized Tandem Photoelectrochemical Cell for Light Driven Total Water Splitting.* Journal of the American Chemical Society, 2015. **137**(28): p. 9153-9159.

205. Renaud, A., et al., *$CuGaO_2$: a promising alternative for NiO in p-type dye solar cells.* Journal of Materials Chemistry, 2012. **22**(29): p. 14353-14356.

206. Iwamoto, S., et al., *Fabrication of Dye-Sensitized Solar Cells with an Open-Circuit Photovoltage of 1 V.* Chemsuschem, 2008. **1**(5): p. 401-403.

207. LIU Qiu-Ping, H.H.-J., ZHOU Yang, DUAN Yan-Dong, SUN Qing-Wen, LIN Yuan, *Photovoltaic Performance of Dye-Sensitized Solar Cells Based on Al-Doped TiO_2 Thin Films.* Acta Phys. -Chim. Sin., 2012. **28**(03): p. 591-595.

208. Daeneke, T., et al., *Dominating Energy Losses in NiO p-Type Dye-Sensitized Solar Cells.* Advanced Energy Materials, 2015. **5**(4).

209. Renaud, A., et al., *Origin of the Black Color of NiO Used as Photocathode in p-Type Dye-Sensitized Solar Cells.* Journal of Physical Chemistry C, 2013. **117**(44): p. 22478-22483.

210. Benko, F.A. and F.P. Koffyberg, *Opto-electronic properties of $CuAlO_2$.* Journal of Physics and Chemistry of Solids, 1984. **45**(1): p. 57-59.

211. Kawazoe, H., et al., *P-type electrical conduction in transparent thin films of $CuAlO_2$.* Nature, 1997. **389**(6654): p. 939-942.

212. Yeap, W.S., et al., *Functionalization of Boron-Doped Nanocrystalline Diamond with N3 Dye Molecules.* Acs Applied Materials & Interfaces, 2014. **6**(13): p. 10322-10329.

213. Huang, Z., et al., *p-Type Dye-Sensitized NiO Solar Cells: A Study by Electrochemical Impedance Spectroscopy.* Journal of Physical Chemistry C, 2011. **115**(50): p. 25109-25114.

214. Devos, A., *The fill factor of a solar-cell from a mathematical point of view.* Solar Cells, 1983. **8**(3): p. 283-296.

215. Altobello, S., et al., *Sensitization of nanocrystalline TiO_2 with black absorbers based on Os and Ru polypyridine complexes.* Journal of the American Chemical Society, 2005. **127**(44): p. 15342-15343.

216. Kinoshita, T., et al., *Enhancement of Near-IR Photoelectric Conversion in Dye-Sensitized Solar Cells Using an Osmium Sensitizer with Strong Spin-Forbidden Transition.* The Journal of Physical Chemistry Letters, 2012. **3**(3): p. 394-398.

217. Feldt, S.M., et al., *Effects of Driving Forces for Recombination and Regeneration on the Photovoltaic Performance of Dye-Sensitized Solar Cells using Cobalt Polypyridine Redox Couples.* Journal of Physical Chemistry C, 2011. **115**(43): p. 21500-21507.

218. Hara, K., et al., *Molecular Design of Coumarin Dyes for Efficient Dye-Sensitized Solar Cells.* The Journal of Physical Chemistry B, 2003. **107**(2): p. 597-606.

219. Cremer, J., *Novel head-to-tail coupled oligo(3-hexylthiophene) derivatives for photovoltaic application*. 2005, University of Ulm: Ulm, Germany.

220. Kirihata, H. and M. Uda, *Externally quenched air counter for low-energy electron emission measurements.* Review of Scientific Instruments, 1981. **52**(1): p. 68-70.

221. He, Y., J. Hu, and Y. Xie, *High-efficiency dye-sensitized solar cells of up to 8.03% by air plasma treatment of ZnO nanostructures.* Chemical Communications, 2015. **51**(90): p. 16229-16232.

222. Abdul Rani, R., et al., *Highly ordered anodized Nb_2O_5 nanochannels for dye-sensitized solar cells.* Electrochemistry Communications, 2014. **40**: p. 20-23.

223. Tan, B., et al., *Zinc Stannate (Zn_2SnO_4) Dye-Sensitized Solar Cells.* Journal of the American Chemical Society, 2007. **129**(14): p. 4162-4163.

224. Sobus, J. and M. Ziolek, *Optimization of absorption bands of dye-sensitized and perovskite tandem solar cells based on loss-in-potential values.* Physical Chemistry Chemical Physics, 2014. **16**(27): p. 14116-14126.